AD

USATRECOM TECHNICAL REPORT 64-54

AN INVESTIGATION OF A DYNAMIC INSTABILITY OF A WINGED GEM

BY
P. M. CONDIT
J. E. HARRINGTON

DECEMBER 1964

U. S. ARMY TRANSPORTATION RESEARCH COMMAND
FORT EUSTIS, VIRGINIA

CONTRACT DA 44-177-AMC-64(T)

PRINCETON UNIVERSITY

DDC Availability Notice

Qualified requesters may obtain copies of this report from DDC.

This report has been furnished to the Department of Commerce for sale to the public.

Reproduction Limitations

Reproduction of this document in whole or in part is prohibited except with permission of the Commanding Officer, USATRECOM. However, DDC is authorized to reproduce the document for United States Government purposes.

Disclaimer

The findings in this report are not to be construed as an official Department of the Army position, unless so designated by other authorized documents.

When Government drawings, specifications, or other data are used for any purpose other than in connection with a definitely related Government procurement operation, the United States Government thereby incurs no responsibility nor any obligation whatsoever; and the fact that the Government may have formulated, furnished, or in any way supplied the said drawings, specifications, or other data is not to be regarded by implication or otherwise as in any manner licensing the holder or any other person or corporation, or conveying any rights or permission, to manufacture, use, or sell any patented invention that may in any way be related thereto.

Disposition Instructions

Destroy this report when it is no longer needed. Do not return it to the originator.

BLANK PAGE

HEADQUARTERS
U S ARMY TRANSPORTATION RESEARCH COMMAND
FORT EUSTIS, VIRGINIA 23604

The investigation described in this report was undertaken to explain the transient dynamic roll instability experienced in the full-scale flight tests (under Contract DA 44-177-TC-850) of a GEM configured for aerodynamic off-loading of the air cushion.

While qualitative airfoil shape and position criteria are established for the fuselage investigated, designs incorporating differing configurations, inlet location, and $C\mu$ will require wind-tunnel analysis to predict whether similar undesirable dynamic conditions will exist. A technique for such an analysis is delineated.

Task 1DO21701AO4802
Contract DA 44-177-AMC-64(T)
USATRECOM Technical Report 64-54
December 1964

AN INVESTIGATION OF A DYNAMIC INSTABILITY OF A WINGED GEM

Report No. 692

by

P. M. Condit and J. E. Harrington

Prepared by
Princeton University
Princeton, New Jersey

for
U.S. ARMY TRANSPORTATION RESEARCH COMMAND
FORT EUSTIS, VIRGINIA

ABSTRACT

This report covers an experimental investigation of the lateral dynamic stability characteristics of a winged GEM. The causes of instability are determined and a method of correcting the condition proposed.

TABLE OF CONTENTS

LIST OF ILLUSTRATIONS

LIST OF ILLUSTRATIONS
continued

LIST OF SYMBOLS

h	height of GEM above ground plane, ft.
mac	mean aerodynamic chord, ft.
C	momentum coefficient ($C = \frac{m_j v_j}{qS}$)
C_L	lift coefficient ($C_L = \frac{W/S}{q}$)
AR	aspect ratio
c.g.	center of gravity
δ	height of wing chord above base of GEM, ft.
mv_j	jet momentum, lbs.
A	lift augmentation ratio ($A = \frac{W}{mv_j}$)
A'	effective lift augmentation ratio ($A' = \frac{W-L_{aero}}{mv_j}$)
W	weight, lbs.
ϕ	angle of roll, degrees
L/D	lift/drag ratio
C_{D_o}	drag coefficient at $= 0^o$
α	angle of attack, degrees
S_j	peripheral jet nozzle area, ft^2
S	GEM base area, ft^2
v_j	jet velocity, ft/sec.
L_{aero}	aerodynamic lift in forward flight, lbs.
D_W	drag of wing in forward flight, lbs.
D_p	parasite drag of GEM, lbs.
D_m	momentum drag, lbs.
$THP_{req.}$	thrust horsepower required
η_p	propeller efficiency
q	dynamic pressure, lbs/ft^2

SUMMARY

The results of experiments looking into the dynamic behavior of winged ground effect machines are presented in a qualitative manner. The work includes smoke tunnel studies and wind tunnel experiments with a dynamic model of a winged GEM. The study was initiated because of an observed dynamic lateral instability during low-speed flight tests of a full-scale winged GEM.

The cause of this instability has been deduced to be related to the circulation-producing effect of a peripheral jet in close proximity to the wing. It is shown that this undesirable behavior can be eliminated by positioning the wing high on the craft and allowing the center of gravity to be located at the midpoint of the mean aerodynamic chord.

INTRODUCTION

During recent years the Princeton group engaged in ground effect machine research has become most interested in the possibilities of improving GEM performance by means of aerodynamic lift.

The spectrum of design possibilities of such a hybrid concept is indeed broad, and after careful consideration it was decided that the most fruitful research could be accomplished by an examination of each end of such a spectrum. This resulted in two separate but related research programs, both of which were sponsored by the U. S. Army Transportation Research Command. They dealt with:

1. The effect of the addition of wings to an otherwise pure GEM.

2. The aerodynamic characteristics of a wingless GEM but one so shaped as to produce favorable aerodynamic forces and moments.

Each of these investigations was both experimental and theoretical, and the experimental portions of both included wind tunnel model testing and full-scale flight testing. The full-scale testing of the winged GEM concept utilized a modified Curtiss-Wright Air Car because of its 60 miles-per-hour top speed capability and because of its availability, while the full-scale flight testing of the shaped GEM idea utilized the Princeton 20-foot circular ground effect machine (P-GEM). Each of these studies indicated the possibility of substantial cruise performance improvement by means of aerodynamic lift. This work is reported in References 1 and 2.

During the course of the full-scale flight tests of the modified and winged Curtiss-Wright ACM-6 Air Car, which is shown in Figure 1, a transient dynamic instability was repeatedly experienced. This instability was not observed in the tests of the original Air Car configuration. Therefore, it appeared that the instability was a function of the addition of wings to the craft, although the real cause could not at that time be deduced.

The nature of the instability was both dynamic and transient. It appeared to be about the longitudinal axis only, producing a rapid and divergent roll oscillation in the speed range of approximately 10 to 20 miles per hour. This roll did not appear to be accompanied by any change in pitch or yaw, nor was the rapid roll present above or below the speed range stated above. The roll was severe in that it became necessary to rapidly accelerate and decelerate through this critical speed range in order to avoid damage to the craft. A typical oscillation would begin quite slowly but would soon increase in magnitude

until the landing pads of the machine would strike the ground with enough impact to cause damage. The rapid roll was also observed at any steady-state speed within the critical range. This behavior of the craft did not seriously affect the test program since the technique of accelerating the craft through this troublesome speed range was quickly developed. The disconcerting fact, however, was that the dynamic instability was not well understood and for that reason might appear at an entirely different speed range in a winged GEM of a different design. For this reason it was deemed advisable to enter into a model study to define the cause of the undesirable behavior and to find a cure for this instability. This report covers the findings of such a study.

DISCUSSION

SMOKE TUNNEL MODEL AND TESTS

In order to determine the cause of the problem stated in the preceding section, it was decided to examine the external aerodynamic flow about a model of the modified Curtiss-Wright Air Car in the Princeton University 3- by 4-foot three-dimensional smoke tunnel.

An existing 1/12th scale powered model of the craft was modified for this phase of the program as shown in Figure 2 and mounted in the smoke tunnel in a manner permitting a wide range of flight attitudes.

The model was tested through a range of yaw angles of $\pm$ 15° and through a range of angles of attack from the minimum to the maximum attainable for each value of the height parameter, $^{h}/_{mac}$. Several values of the height parameter were examined, extending from $^{h}/_{mac}$ = .02 to $^{h}/_{mac}$ =.15. The model was tested both fixed in roll and free in roll. The maximum roll angles were limited to those possible for the particular value of $^{h}/_{mac}$.

The technique employed in these flow visualization experiments was to introduce smoke into the tunnel external of the model at approximately one model length upstream. The position of the smoke injector was varied in an attempt to define all gross flows about the model. Observations including photographs were made through windows on both the top and the sides of the test section and through a porthole downstream of the model. The momentum coefficient, C_μ, was varied by changing tunnel speed for a fixed value of model power for one series of tests and by changing model power for a fixed value of tunnel speed in another series of experiments. Both of these techniques yielded identical results as discussed below.

TEST RESULTS

Figure 3 shows a selected group of the most pertinent photographs taken in the smoke tunnel. Close study of these photographs resulted in the information necessary to construct the diagrams of Figure 4. Since the dominant aerodynamic flow seemed to be invariant with the height parameter through a modest range of $^{h}/_{mac}$, a rather high value was selected for detailed study for the sake of convenience. Also, since the flow characteristics seemed to be dependent only upon C_μ, it was found most convenient, to set the wind tunnel speed and to vary only model power. It will be noted from an examination of both Figures 3 and 4 that the character of the flow is strongly a function of C_μ. Figure 4-a shows the general flow about the wing for a low value of C_μ (i.e., low model power).

A higher value of model power at the same forward speed caused the flow to change in a manner shown in Figure 4-b. This is comparable to a high value of C_μ . Additional model power produced a further change in the flow as shown in Figure 4-c. Thus, the flow patterns of Figure 4 are related to C_μ in the following general manner:

Figure 4-a - moderate C
Figure 4-b - high C
Figure 4-c - very high C

By noting the position of the leading edge stagnation point for each of these flow conditions, it is readily seen that the wing lift coefficient undergoes a severe change with this change in C_μ . It was also observed that the flow conditions of Figures 4-b and 4-c could be alternately produced through the incremental C_μ range required for each flow. That is, a very definite C_μ range exists which permits the flow to vary from that shown in Figure 4-c to that of Figure 4-b. Further, this flow is asymmetric relative to the model through a finite C_μ range. This means that during an acceleration and again during a deceleration, a C_μ range is passed through which first produces the conditions of Figure 4-c on one wing while the flow of Figure 4-b exists on the opposite wing of the craft. An instant later, the flow conditions may reverse. This, of course, produces a strong rolling moment which would create lateral oscillation in a free-flight craft. Thus, the flow patterns producing the alternating lift forces seem to be defined. The exact mechanics of the combined peripheral jet efflux and the free-stream velocities in producing these resultant flows is, however, a matter of some speculation. A possible explanation, and one that seems reasonable in light of the results of the vast amount of research conducted in the past with circulation control systems, is presented below.

It is necessary to consider the peripheral jet in close physical relationship to the wing as a circulation control device. As such, the momentum coefficient C_μ would be infinitely high during the hovering flight of the hybrid craft and would diminish to lower finite values as the forward speed of the machine is increased. The variation of incremental lift coefficients with C_μ is, however, very analogous to the variation of lift coefficient with angle of attack of a fixed wing. This ΔC_L, C_μ relationship is shown in a general way in the diagram below:

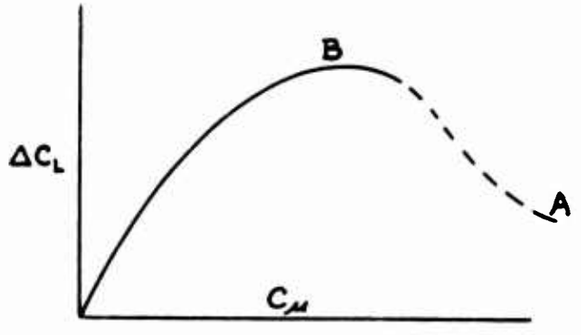

In general, circulation is increased with increasing C_μ until at some point the circulation reaches a magnitude that the wing cannot support. At this point there is a definite decrease in ΔC_L with increasing values of C_μ . The initial slope of the curve ($d\Delta C_L/dC_\mu$), the nature of the top of the curve (whether it be continuous or show a strong discontinuity), and the character of the curve after this point are functions of the geometry of the system. The diagram shown, however, can be considered a very general presentation of the typical behavior of a blowing circulation control system.

The point B can be considered a momentum coefficient stall. It is the point beyond which the leading edge of the airfoil cannot remain attached due to the supercirculation.

In the case of the winged GEM it appears that the very high values of C_μ at very low forward speeds cause the flow shown in Figure 4-c, which would be on the portion of the curve labeled A in the Figure. As the forward speed of the craft increases, C_μ decreases, causing the ΔC_L to maximize as shown in Figure 4-b. This corresponds to point B on the diagram.

Since it is not possible to construct any craft, whether it be model or full scale, precisely symmetrical in all respects, including not only its geometry but also the distribution of the jet efflux (in the case of a peripheral jet machine), it is reasonable to expect that as point B is approached, one wing will attach prior to the other. Thus a rolling moment is generated due to the asymmetric span lift distribution, which in turn produces an asymmetric downwash distribution and can influence the jet efflux to the extent of completely reversing the span lift distribution at this critical and unstable point B. Also, it could be reasonably argued that the physical roll of a free-flight craft would influence the jet efflux distribution, which at the critical point B would cause the asymmetric span lift distribution to reverse itself. These smoke tunnel findings and the above deductions are offered for the consideration of others. They are the authors' best opinions based upon the facts revealed during the study.

THE DYNAMIC MODEL

Two philosophies were considered in the determination of the general configuration of the dynamic model. The first, for the sake of consistency, was the advisability of designing a model geometrically and dynamically similar to the winged version of the Curtiss-Wright Air Car. The second approach, and the one adopted, was based upon the fact that the dynamic model should be a state-of-the-art winged GEM. Since the findings of the smoke tunnel experiments did not indicate that the behavior of the model was strictly limited to the

exact geometry of the machine which first experienced the dynamic instability, it was felt that some desirable changes in configuration could be tolerated without jeopardizing the validity of the over-all study.

The purpose of the dynamic model was to simulate the dynamic behavior of the full-scale winged GEM and, more importantly, to find a satisfactory cure for the lateral instability problem.

For the reasons mentioned above, it was decided to base the dynamic model upon a design of an optimized winged GEM - optimized, that is, to the extent of the knowledge in hand of this type of hybrid craft. This philosophy and the preliminary design of the full-scale craft are presented in the Appendix of this report. The model itself was a 1/12 scale model of this design, and its geometry and mounting arrangements are shown in Figure 5; a photograph of the model is shown in Figure 6. It will be noted in Figure 5 that the model was equipped with two sets of wings, one with a straight leading edge and the other with a 45^{o} swept leading edge. Both wings are of the same area, span and aspect ratio. These wings were mountable in two longitudinal positions (i.e., c.g. @ 0% mac and c.g. @ .25 mac) in addition to being movable to three vertical positions on the craft. It will be noted from an inspection of Figure 5 that the aspect ratio of both sets of wings was 2.2 and that the airfoil section was NACA 23012 profile.

DYNAMIC TESTS

The dynamic model was mounted in the Princeton University 2- by 3-foot three-dimensional wind tunnel above a ground plane of the same area as the floor of the test section. The model was free in roll, pitch and yaw and was adjustable vertically for the various values of h/mac desired. Many preliminary tests were run to check out the behavior of the craft through a wide range of variables in order to determine those of most significance. From these tests it was determined that the following range of variables would most probably define the general dynamic behavior of the winged GEM concept:

1. Two values of model power
2. Accelerating and decelerating forward speed
3. Two values of h/mac ($h/mac = .025$ and $.05$)
4. Two longitudinal positions of the wing (c.g. @ .25 mac and c.g. @ .00 mac)
5. Two vertical positions of the wing ($\delta/mac = .10$ and $\delta/mac = .35$)

It was also decided to repeat the experiments looking into the above set of variables for each of three configurations:

1. No wings
2. Straight wings
3. Swept wings

The model was tested by first applying the desired model power and then starting the wind tunnel and slowly increasing the speed of the air through the test section. It was subsequently found, however, that much smoother decelerations could be accomplished than was the case for positive acceleration. Since the full-scale craft had shown the undesirable rapid roll in both cases, it was decided to concentrate the major attention on decelerating flight. Sensing of all dynamic motion of the model was accomplished by means of micro-torque potentiometers attached to the gimble assembly within the model, and read-out was by means of a four-channel Carrier amplifier and recorder. Test section velocity was sensed by a calibrated axial flow fan in the free stream driving a micro-torque generator also reading out through the same amplifier and recorder.

DYNAMIC TEST RESULTS

The most significant results of these tests are shown in Figures 7 through 20. These figures cover a range of test conditions which seems to define completely the importance of each of the variables studied. It will be noted that each figure is assigned a code number which by reference to the table of Figure 21 describes the conditions of each experiment. It will be noted that the lowest trace on each of the Figures 7 through 20 is the velocity record. One millimeter of displacement of this curve equals 1.9 ft/sec of velocity.

Of importance in interpreting these results is the fact that wherever dutch roll occurs, there will be a corresponding oscillation in yaw. This is, however, distinctly different from the rapid roll experienced with the full-scale craft. An example of this is the dutch roll mode shown in Figures 7 and 8. It appears that for this case (the wingless craft), there is no unrelated rapid roll since all roll is accompanied by a distinct and severe yaw oscillation. This motion seems to be independent of C_μ . These general statements appear valid also for the case of variations of the height parameter. This results from a comparison of Figures 8 and 9, again for the wingless craft.

For the case of the high swept wing at a high C_μ , it can be seen by comparing Figures 10 and 11 that at the higher value of $^h/_{mac}$ the dutch roll is present, but for a reduced value of $^h/_{mac}$ the dutch roll is damped and a rapid roll is experienced.

The effect of varying the longitudinal position of the wing on the model is shown in a comparison of Figures 11 and 12. It will be noted by inspection of these traces that the dutch roll has essentially disappeared, but for both cases a rapid roll persists.

In order to determine the general effect of the vertical position of the swept wing, Figures 12 and 13 are compared. It is seen from these figures that the high wing position produced rapid roll only, while the lower position produces both rapid roll and dutch roll. For this same wing mounted in a low position, it is seen from inspection of Figures 13 and 14 that the effect of reducing C_{μ} is to eliminate the dutch roll tendency, leaving only the rapid roll characteristics.

For the case of the high straight wing, Figures 15 and 16 may be compared. It will be noted that for the low C_{μ} test, a pronounced dutch roll was experienced; however, when C_{μ} was increased, the roll oscillation became predominantly of the rapid type with little of the dutch roll motion. By further comparison with Figure 17, it is seen that by moving the wing closer to the base of the machine, the dutch roll once again becomes the dominant dynamic characteristic.

The effect of c.g. position relative to the mean aerodynamic chord can be determined from Figures 17 and 18. It will be noted that dutch roll characteristics seem to disappear with an aft movement of the c.g.; however, rapid roll continues for this configuration. Further comparison with Figure 19 shows a return of the dutch roll mode with a reduction of the height parameter h/mac.

It appears from these experiments that the straight wing is generally superior to the swept wing and that the most favorable position of the wing is the higher position. Also, it appears that the position of the c.g. is quite important, the aft location being the more favorable. As a consequence of these findings, an additional configuration was tested embodying all of the advantageous geometric parameters found from the experiments discussed above. This final configuration included a higher wing position (δ /mac = .45), and the c.g. moved aft to 50 percent of the mean aerodynamic chord. The results of tests with this arrangement are shown in Figure 20. It will be noted that all rapid roll has vanished, as has the previously noted strong dutch roll tendency.

Therefore, it appears that the solution to the problem of dynamic roll irstability of a winged GEM is geometric design, the most important aspect of which is to remove the wing from the vicinity of the base of the ground effect machine. These dynamic findings seem to agree with those of the smoke tunnel study.

CONCLUSIONS

This study has been a qualitative one, intended to provide an understanding of the causes of an observed dynamic instability of a winged ground effect machine. Further, the research was directed toward finding a general solution to this instability. Careful consideration of the results of these experiments seems to justify the following conclusions:

1. A peripheral-jet ground effect machine can become dynamically unstable about the longitudinal axis at low values of forward speed, with the addition of wings near the base of the craft. This instability will generally disappear at higher airspeeds.

2. The cause of this instability appears to be associated with the circulation-producing effect of the peripheral jet in close proximity of the wing.

3. The magnitude and mode of this dynamic instability can be influenced by the planform of the wing, its vertical position on the craft, and the position of the center of gravity relative to the mean aerodynamic chord of the wing.

4. It was found that an unswept wing mounted high on the GEM with an aft location of the c.g. provided a general solution to the problem. It was determined that the optimum location of the wing was δ /mac = .45 and that the most desirable position of the center of gravity was 50 percent of the mean aerodynamic chord.

REFERENCES

1. Summers, D. R., Carr, G. P., Metzko, J. J., Nixon, W. B. and Wojciechowicz, A. F., Jr., The General Characteristics of Winged Ground Effect Machines, TRECOM Report 63-36, October 1963.

2. Wojciechowicz, A. F., Jr., Nixon, W. B., and Sweeney, T. E., The Dominant Aerodynamic Characteristics of a Shaped GEM, TRECOM Report 64-45 (in publication).

3. Sweeney, T. E. and Nixon, W. B., Planform Characteristics of Peripheral Jet Wings, Princeton University Aero. Report No. 524, December 1961.

4. Fuik, M. P., Lastinger, J. L., Aerodynamic Characteristics of Low Aspect Ratio Wings in Close Proximity to the Ground, NASA T.N. D926, July 1961.

BLANK PAGE

DISTRIBUTION

US Army Materiel Command	3
US Army Mobility Command	4
US Army Aviation Materiel Command	5
US Strike Command	1
Chief of R&D, DA	3
US Army Transportation Research Command	63
US Army Research and Development Group (Europe)	2
US Army Engineer Research and Development Laboratories	4
US Army Limited War Laboratory	1
US Army Human Engineering Laboratories	1
Army Research Office-Durham	2
US Army Research Support Group	1
US Army Medical Research and Development Command	1
US Army Engineer Waterways Experiment Station	1
US Army Combat Developments Command Transportation Agency	1
US Army War College	1
US Army Command and General Staff College	1
US Army Transporation School	1
US Army Tank-Automotive Center	2
US Army Arctic Test Center	1
US Army General Equipment Test Activity	1
US Army Airborne, Electronics and Special Warfare Board	1
Chief of Naval Operations	1
Bureau of Ships	1
Bureau of Naval Weapons	2
Bureau of Supplies and Accounts, ND	1
US Naval Postgraduate School	1
David Taylor Model Basin	1
Marine Corps Landing Force Development Center	1
Marine Corps Educational Center	1
Marine Corps Liaison Officer, US Army Transportation School	1
Ames Research Center, NASA	2
NASA-LRC, Langley Station	2
Lewis Research Center, NASA	2
NASA Representative, Scientific and Technical Information Facility	2
Human Resources Research Office	2
US Army Standardization Group, Canada	2

Canadian Liaison Officer,	
U. S. Army Transportation School	3
British Army Staff, British Embassy, Washington	4
U. S. Army Standardization Group, U. K.	1
Defense Documentation Center	20
U. S. Government Printing Office	1

APPENDIX

A PRELIMINARY DESIGN STUDY OF AN OPTIMIZED WINGED GEM

1. DESIGN PHILOSOPHY

The design criteria for such a craft as outlined here was arrived at by a conference with Mr. William Sickles and Mr. William Hinshaw of TRECOM late in 1962.

It was decided that the design would strive to achieve the following performance characteristics:

a) 1-ton payload
b) 8-inch hover height
c) 2-foot cruise height
d) 70-knot cruise
e) 2 hours endurance at full throttle
f) exceptional maneuverability

In addition, it was decided that the width of the machine could not exceed 10 feet 3 inches in order that it be air transportable. It will be noted in Figure 22 that this requirement is met by assuming the wing to be removable or retractable.

The craft has been conceived to be as light as possible; however, because of size limitations and payload requirements, the base loading is unfortunately about twice that deemed optimum. But it is substantially reduced at cruise speed by the lift of the wings.

2. PRELIMINARY WEIGHT ANALYSIS

Structure	1200 lbs.
Propulsion Engine Allison T-63, 250 SHP	150 lbs.
Lift Engine Airesearch M 331, 456 SHP	200 lbs.
Fuel (2 hours) (with 30 min. reserve)	1150 lbs.
Wing	200 lbs.

Payload - - - - - - - - - - - - - - - - -	2000 lbs.
Control System - - - - - - - - - - - - -	100 lbs.
Design Gross Weight - - - - -	5000 lbs.

3. PERFORMANCE ESTIMATION

The performance estimation for the optimized winged GEM was carried out in two parts, one to determine the craft's characteristics as a pure GEM and a second to determine its cruise characteristics as a winged GEM.

A) Pure GEM

From Reference 3, the static lift augmentation curve shown in Figure 23 was deduced from previous experimental results. For the 5000 pounds gross weight condition and assuming mv_j = 2 pounds/brake horsepower, the static lift augmentation would have to be approximately 5.55. This yields a hover height at 100 percent throttle of .12 $^{h}/_{w}$, or approximately 1.2 feet. Since this is considerably higher than that required, it was at first thought wise to select a lower power lift engine; however, experience has shown that the availability of additional power is highly desirable in GEM operation. The question of the lateral static stability of the craft in the pure GEM condition, particularly at its maximum hover height of 1.2 feet, was expected to be solved by the addition of a single longitudinal compartmentation slot. But it was felt that the compartmentation slot would not be necessary since the craft is unstable through only a small angular range, becoming neutrally stable at $\emptyset = \pm 4^{o}$ and rapidly increasing in static stability with increasing angle of roll. Since the machine would have a maximum hovering roll angle capability of at least 11^{o}, it was felt that the inherent stability of the base configuration would be adequate. If this proves to be inadequate, there is enough power available to add a compartmentation slot and still meet the hover requirement of 8 inches. There appears to be no longitudinal static stability problem.

B) Winged GEM Condition

By inspection of Figure 22, with its rather arbitrary vertical position of the wing, it was decided that at a cruise height of 2 feet the mac would be approximately .66 mac above the ground. From Reference 4 it was determined by interpolation that this aspect ratio of 2.7 wing should have an L/D max. of approximately 11.5 at $^{h}/_{mac}$ = .66 and a lift coefficient = 0.6.

In order to arrive at a reasonable value of total wing lift coefficient, a 33 percent carry-over of lift through the body of the craft was assumed. This is always a difficult value to determine. It is obvious, however, that lift will not fall to zero at the wing root unless there is a wide gap; it is also obvious that the profile of the craft is substantially less effective as a wing than the wing panels themselves. Therefore, it appears reasonable that this value of 33 percent carry-over cannot be far from the truth. To further substantiate this assumption, reference is made to the Princeton Winged GEM Final Report No. 657, which indicates that this value of carry-over appeared valid for the full-scale Curtiss-Wright Air Car flight results. At any rate, a weighted average lift coefficient for the entire wing appears to be approximately 0.4 based upon 150 ft^2 of wing immersed in the body of the GEM and 180 ft^2 of wing in the free stream.

It was further assumed that a momentum drag recovery of 33 percent could be achieved by means of adjustable or, possibly, fixed vanes in the side nozzles of the craft. However, there has been considerable disappointment experienced by GEM designers in the amount of mv_j recovery due to θ vanes. For that reason and because the assumed value of thrust propeller efficiency of .8 may be optimistically high, the performance computations do not include any momentum drag recovery.

Additional information required before actual performance computations could be made was a fairly accurate estimation of the craft's form drag, minus wings. This was obtained from the unpublished wind tunnel results shown in Figure 24. These tests were conducted at Princeton during the summer of 1962 to aid in the analysis of the winged GEM studies then underway.

Figure 24 clearly shows the beneficial effect of fairing the nose and tail of an otherwise box-shaped GEM. Since the machine is similar in profile to the faired version of the Curtiss-Wright Air Car, a value of C_{Do} of 0.07 was assumed at $\alpha = 0^o$ for the former machine.

From the geometry of the base ($S_j/S = .1$) and from the assumed value of 900 pounds of full throttle mv_j , v_j was determined to be 135 ft/sec and m = 6.7 lbs sec/ft.

The foregoing assumptions and information yield the following table:

$V_{KTS.}$	V_{mph}	$V_{ft/sec}$	L_{AERO} lbs.	D_W lbs.	D_P lbs.	D_M lbs.	D_T lbs.	$THP_{REQ.}$	L_{BASE} lbs.	A	$h/_w$	$h_{ft.}$
0	0	0	0	0	0	0	0	0	5000	5 55	.12	1.2
12	13.5	20	63	5.5	1.0	135	141	5	4940	5.5	.125	1.25
23	27	40	250	22	4.4	270	297	22	4750	5 3	.130	1.30
36	41	60	570	50	9.8	400	460	50	4430	4.8	.150	1.50
48	55	80	1000	87	17.5	540	644	94	4000	4.4	.170	1.70
59	68	100	1580	137	27	670	834	152	3420	3.8	.210	2.10
71	81.5	120	2300	200	39	800	1040	230	2700	3.0	.30	3.00

From the results of these computations, curves shown in Figures 25 and 26 were constructed. Figure 25 shows the effect of the wings in permitting the craft to fly at lower lift augmentation ratios with increased forward speed. From this figure values of A' were taken for selected speeds, and these values of A' were converted to h/w by means of Figure 23. This procedure yielded the height-versus-velocity curve shown in Figure 26. Also shown on Figure 26 is the thrust-horsepower-required curve. The Allison T-63 gas turbine was selected as the propulsion engine. This engine has a full-throttle power of 250 brake horsepower and, considering a propeller efficiency of η_p = 0.8, it appears that 200 thrust horsepower might be attained at that power setting.

In summary, the performance of the craft is as follows:

Hover height - - - - - - - - - - - - - - - 1.2 ft.

V max. - - - - - - - - - - - - - - - - - - - 67 kts.

Height at V max. - - - - - - - - - - - - - 2.6 ft.

Lift power, Airesearch M 331 - - - - - - - 450 BHP

Thrust power, Allison T-63 - - - - - - - - 250 BHP

Endurance at full throttle - - - - - - - - 2 hrs.

Payload - - - - - - - - - - - - - - - - - -2000 lbs.

4. CONTROL SYSTEM

It has become apparent over the years that a GEM, particularly one with high ground clearance, must have attitude control about all three axes. This attitude control, while important for trim, also provides optimum maneuvering forces at low speeds. It is suggested that this be accomplished by spoilers or throttling vanes in the peripheral nozzle. Directional control would be accomplished by mounting the thrust engine (at its c.g.) on a swiveling mount.

Control at cruise speeds and above would be by means of air rudders, a horizontal trimmer spanning the twin fins, and ailerons on the wing. Braking would be accomplished by means of a reversible propeller on the thrust engine and, if necessary, controllable β vanes. Figure 27 shows the general arrangement of a proposed dynamic wind tunnel model of this craft. No dimensions are shown in Figure 27 because it has not yet been determined which of the Princeton tunnels will be used for the experiments. It will be noted that the model is electrically powered, with the motor located at the c.g. The mounting system, permitting three degrees of freedom, is fastened to the model at the c.g. by means of a yoke which surrounds the motor. Also shown are three vertical positions of the wing, two planforms, and two longitudinal wing positions. Roll, pitch and yaw displacements will be sensed by micropotentiometers of each axis and recorded on a three-channel recorder for each of several airspeeds, geometric configurations, and ground clearances.

FIGURE 1. Full Scale Winged GEM (Modified C-W Air Car).

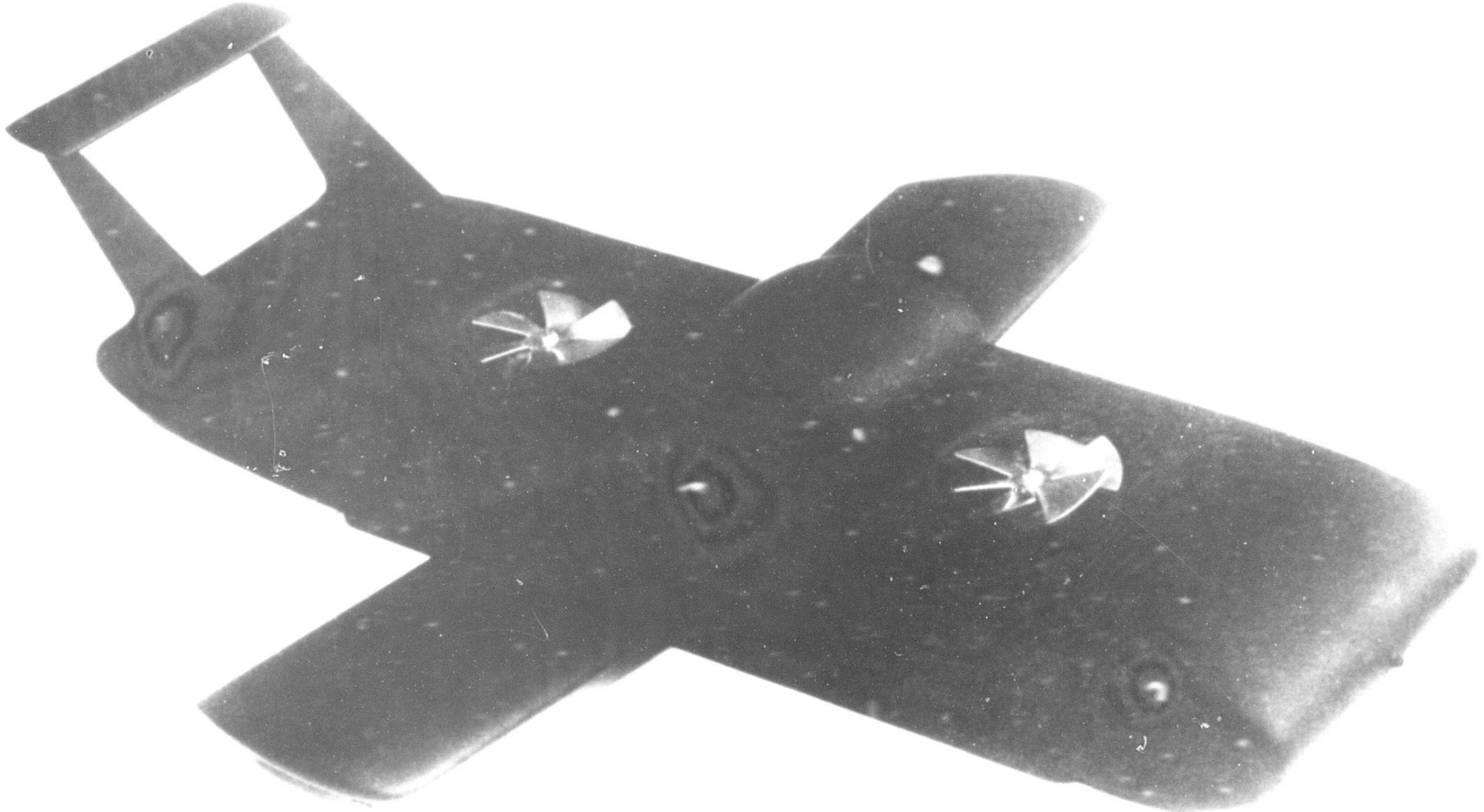

FIGURE 2. Wind Tunnel Model (Modified C-W Air Car).

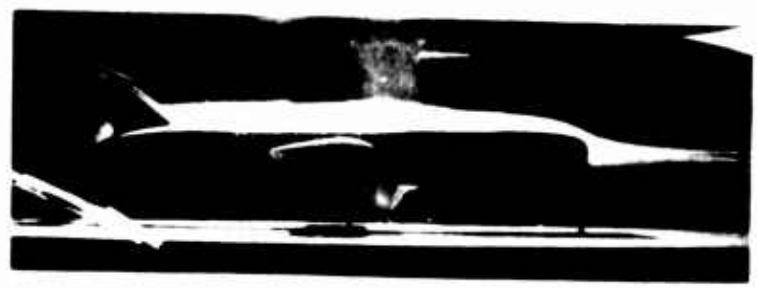

FLOW PATTERN ABOVE MODEL

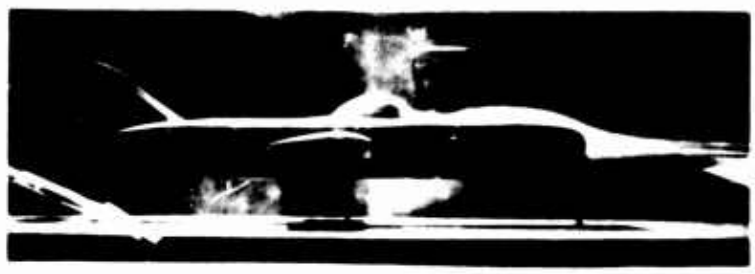

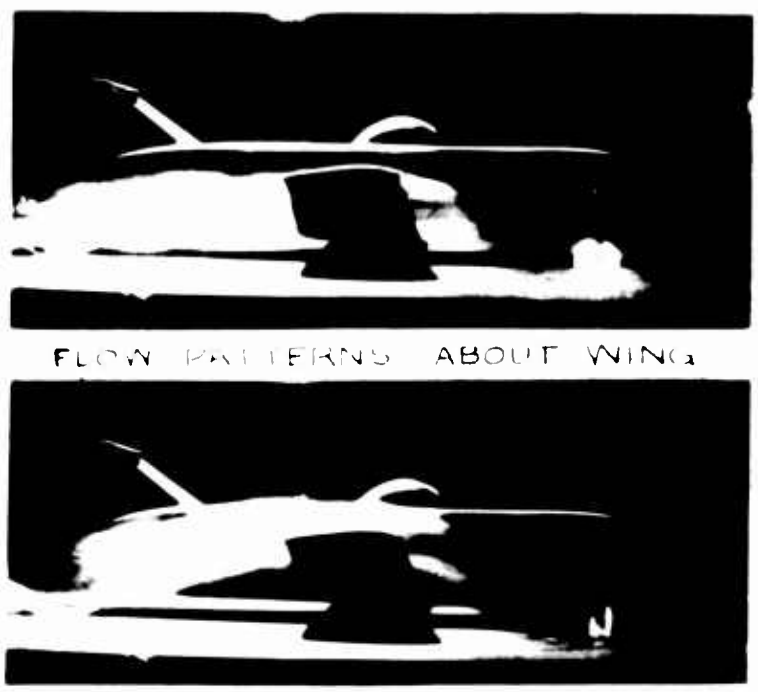

FLOW PATTERNS ABOUT WING

FIGURE 3. Smoke Flow Studies About Winged GEM Model.

$C_\mu = 0$

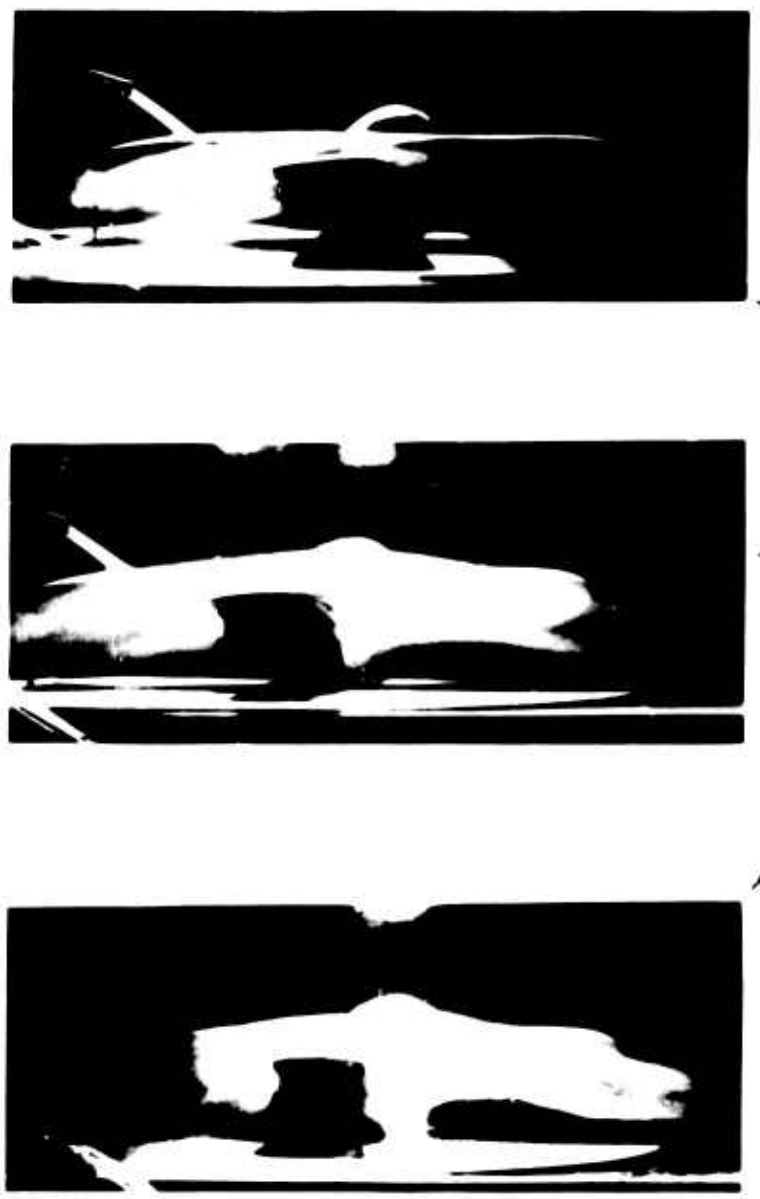

VERY HIGH C_μ

FIGURE 3 contd. Smoke Flow Studies About Winged GEM Model.

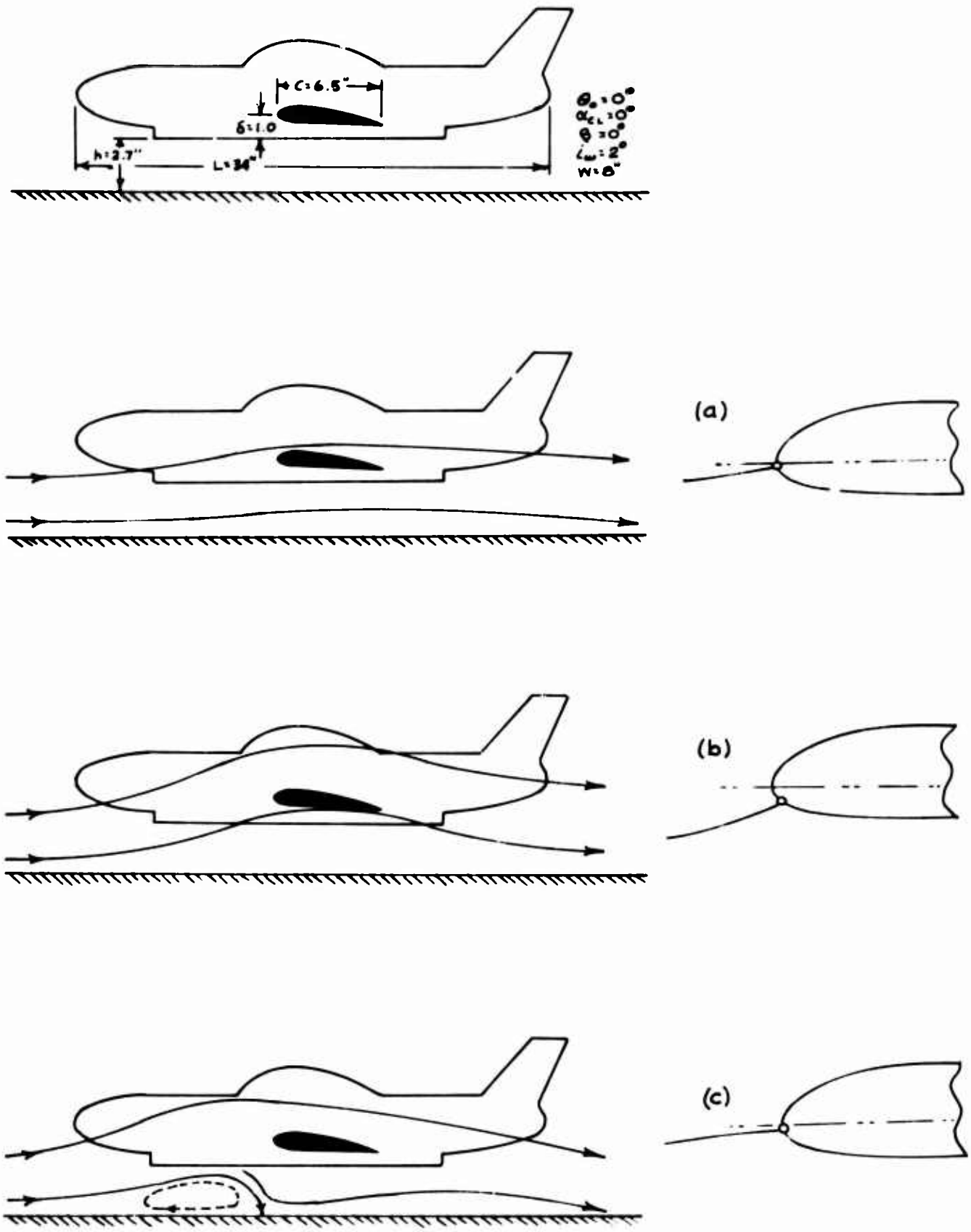

FIGURE 4. Position of Leading Edge Stagnation Point as Function of C_μ .

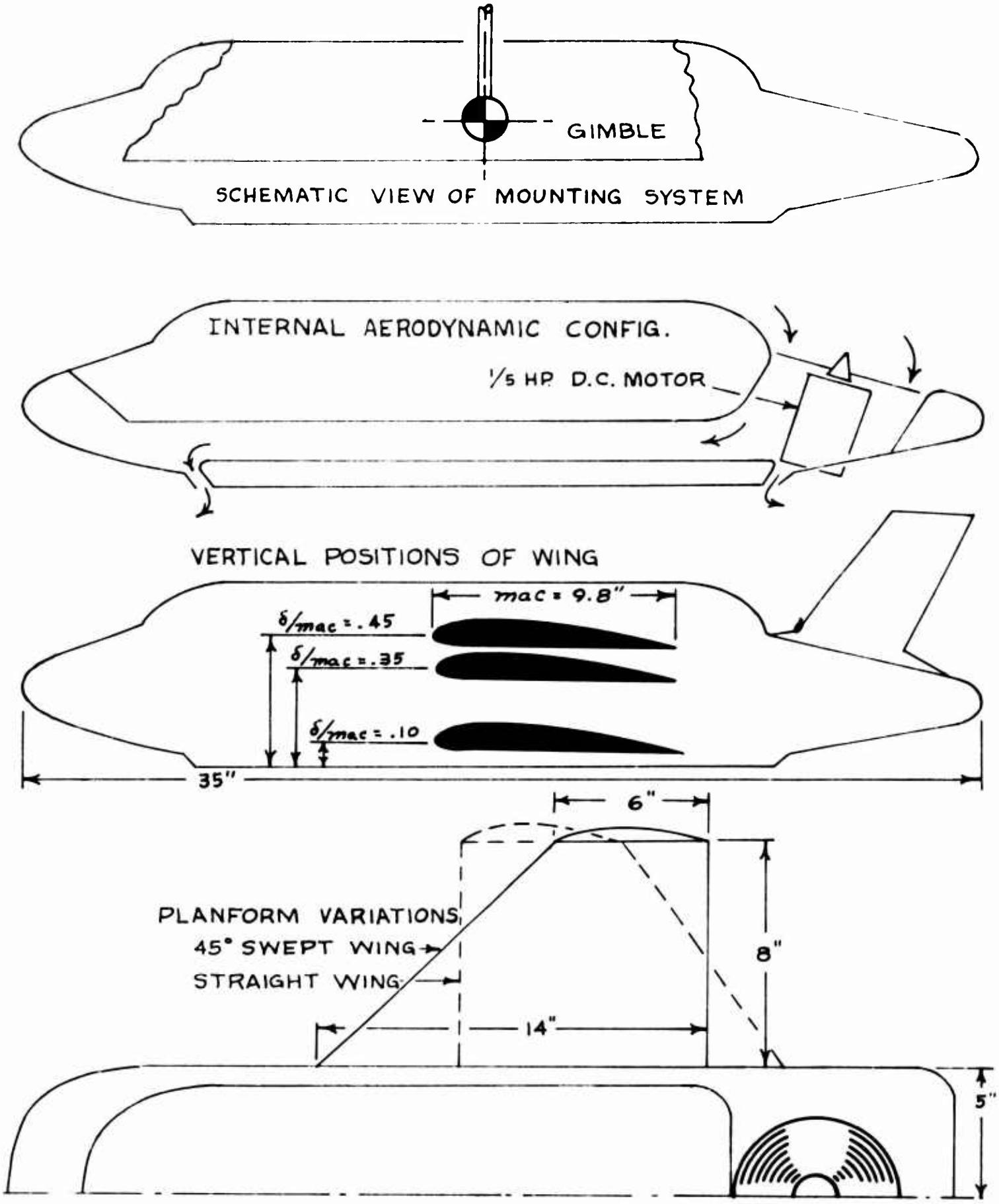

FIGURE 5. General Characteristics of Dynamic Model.

FIGURE 6. Dynamic Wind Tunnel Model of Winged GEM.

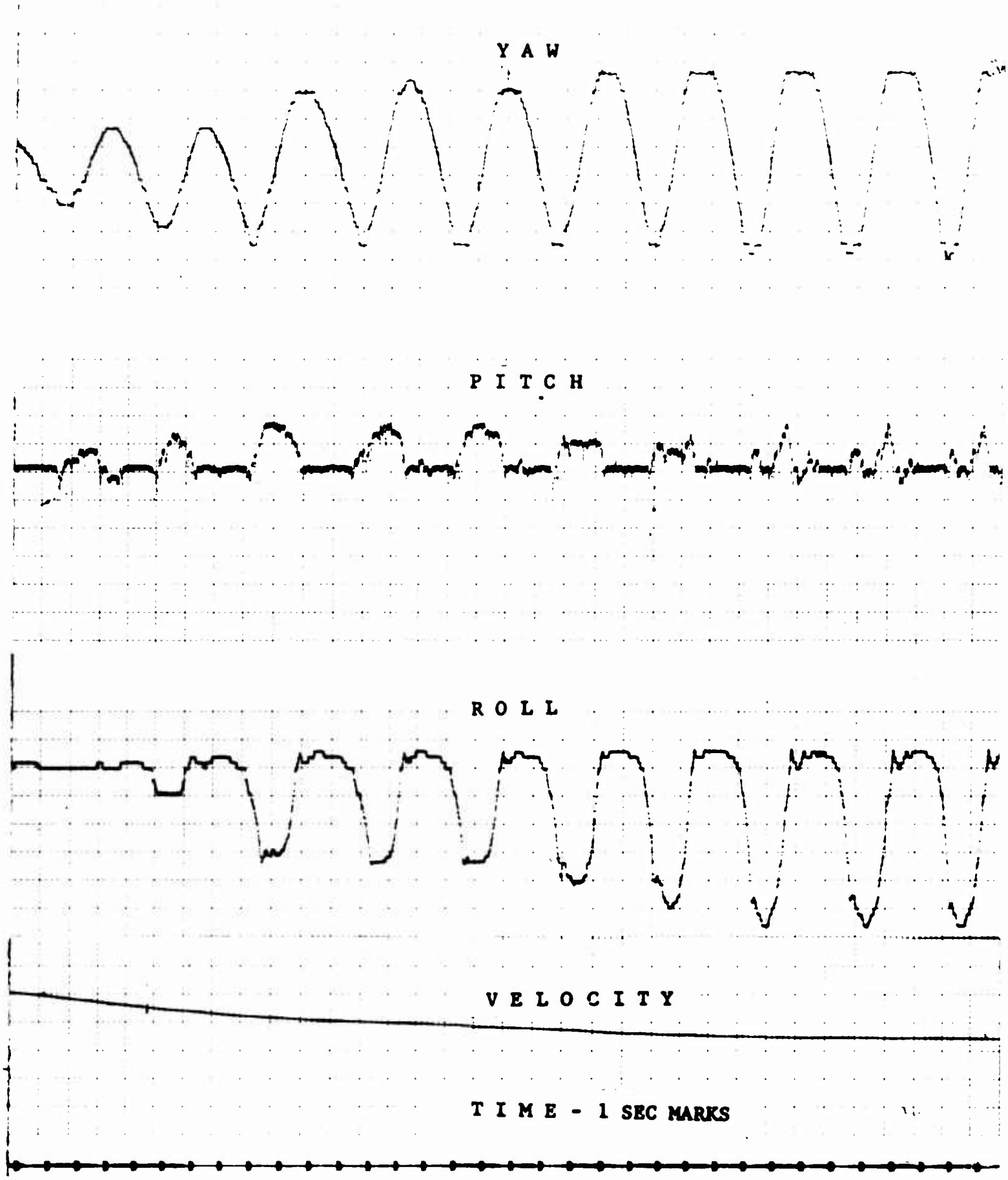

FIGURE 7. Dynamic Behavior of Winged GEM Model - Code 1.

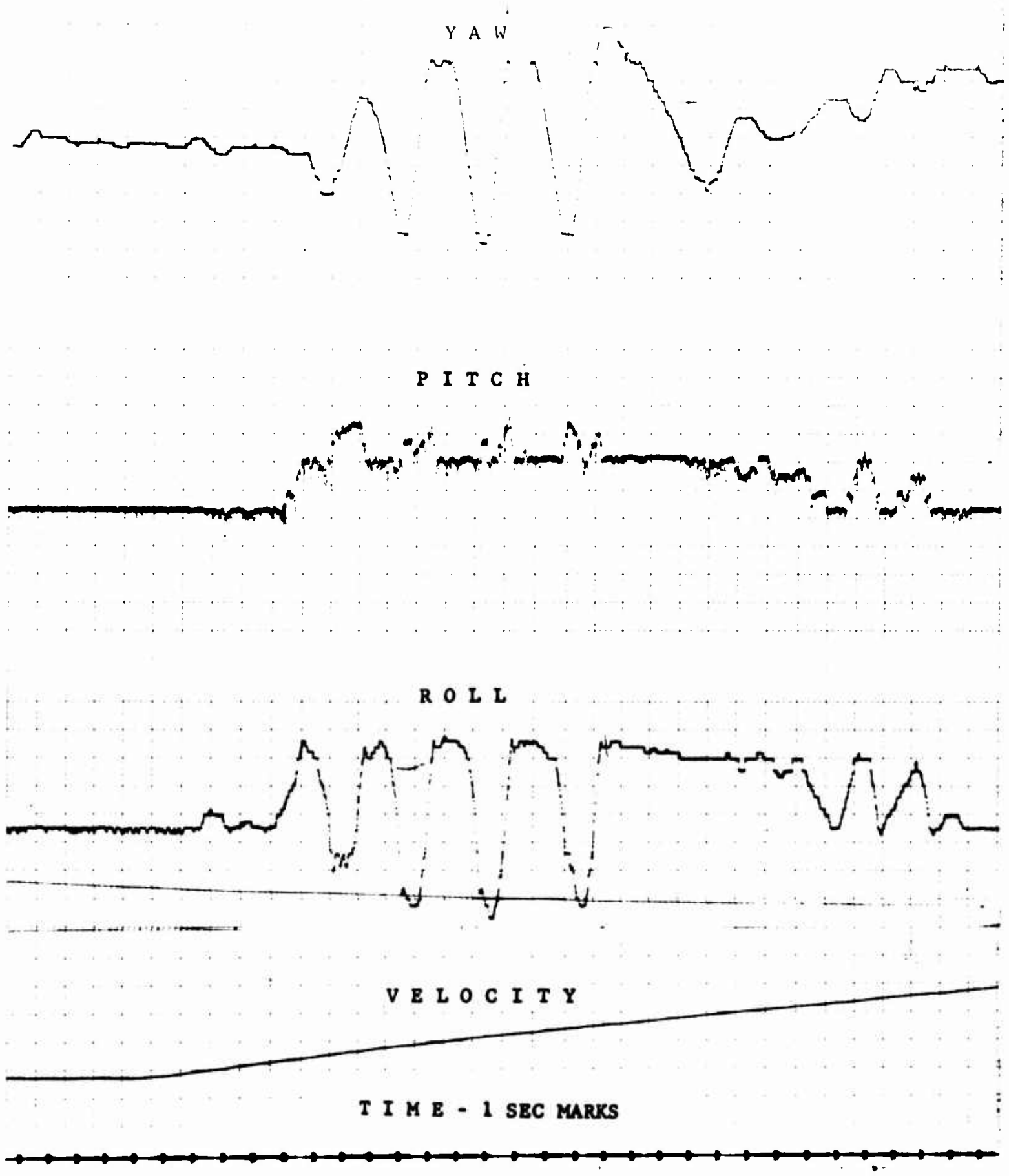

FIGURE 8. Dynamic Behavior of Winged GEM Model - Code 2.

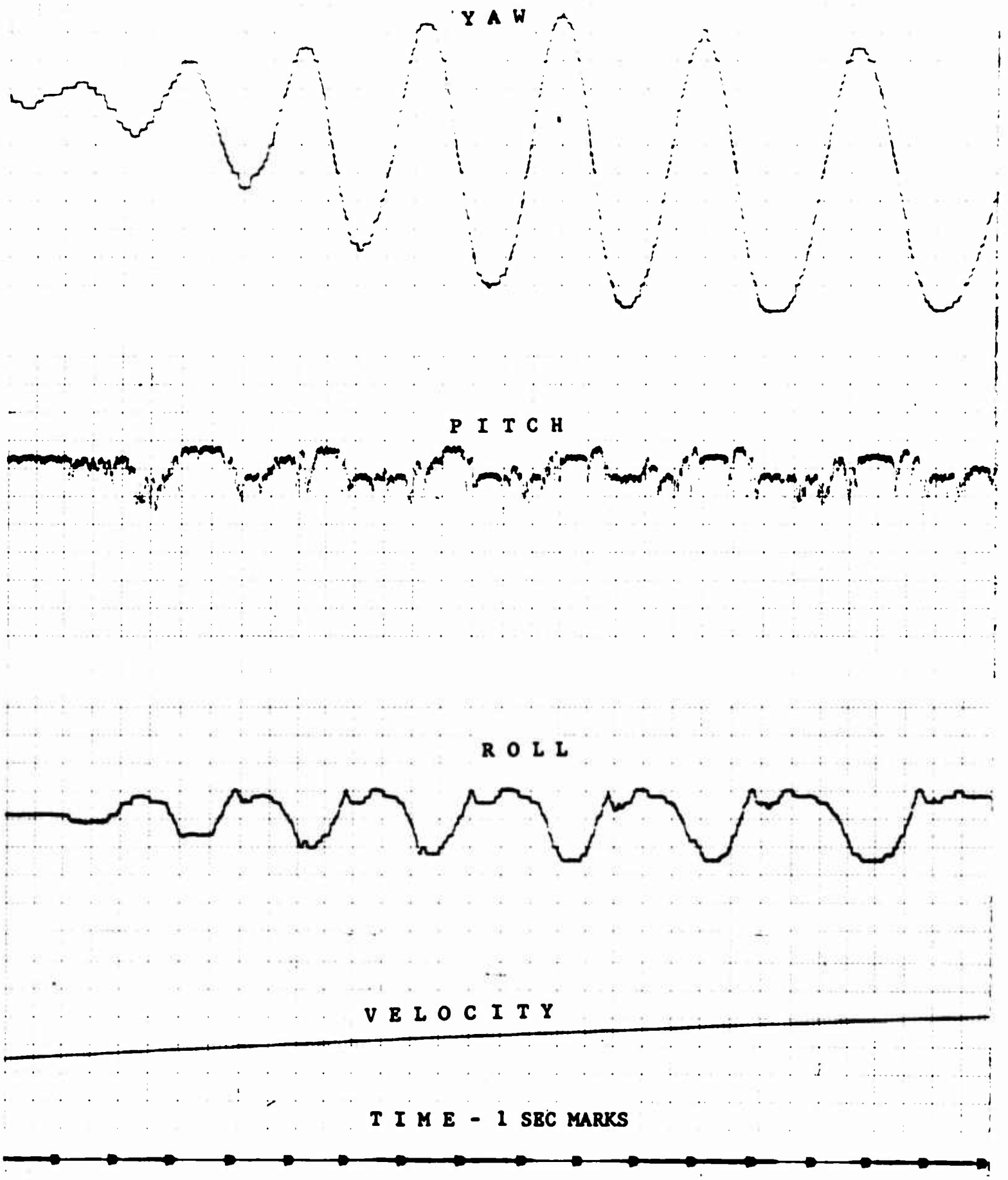

FIGURE 9. Dynamic Behavior of Winged GEM Model - Code 3.

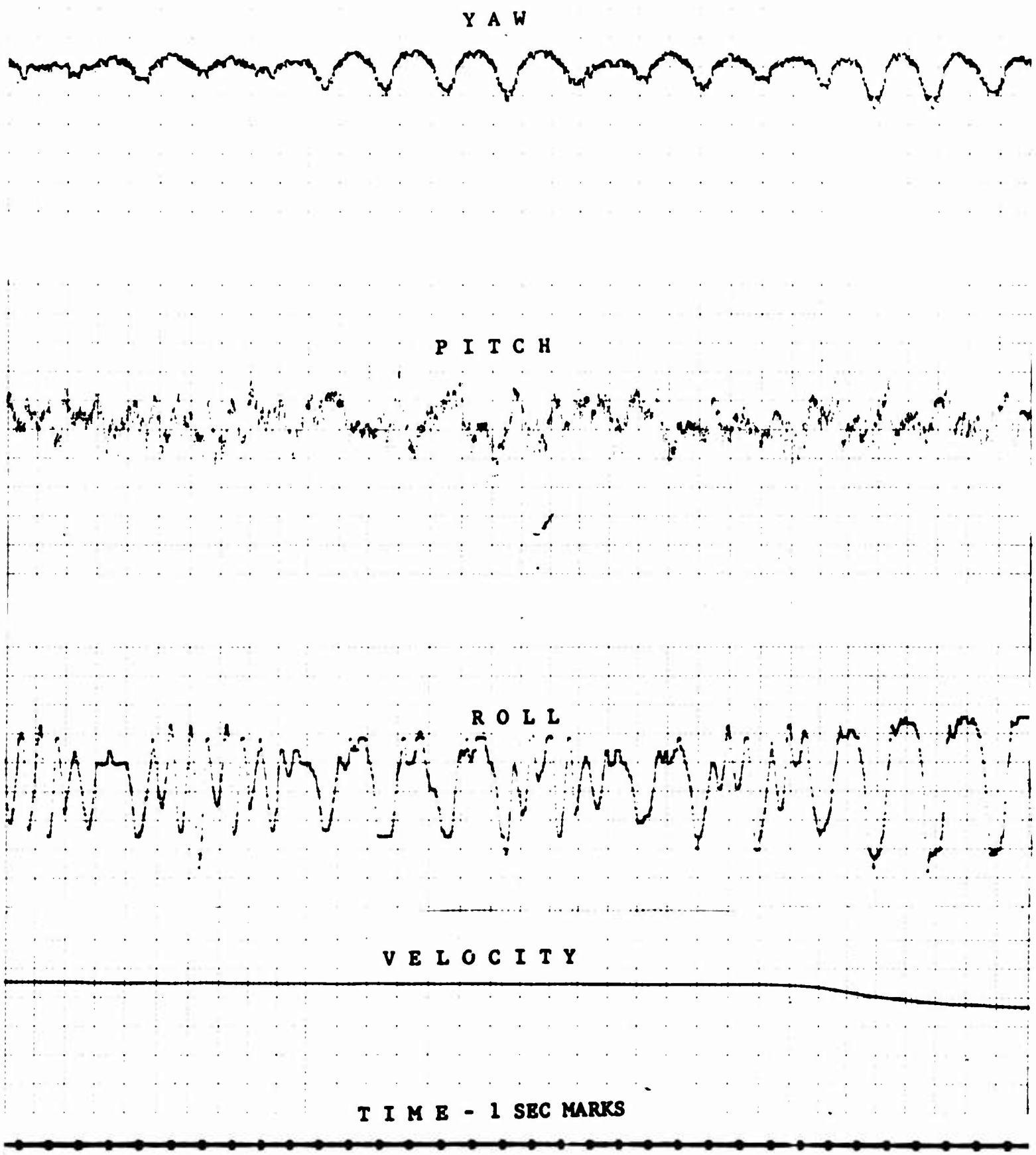

FIGURE 10. Dynamic Behavior of Winged GEM Model - Code 4.

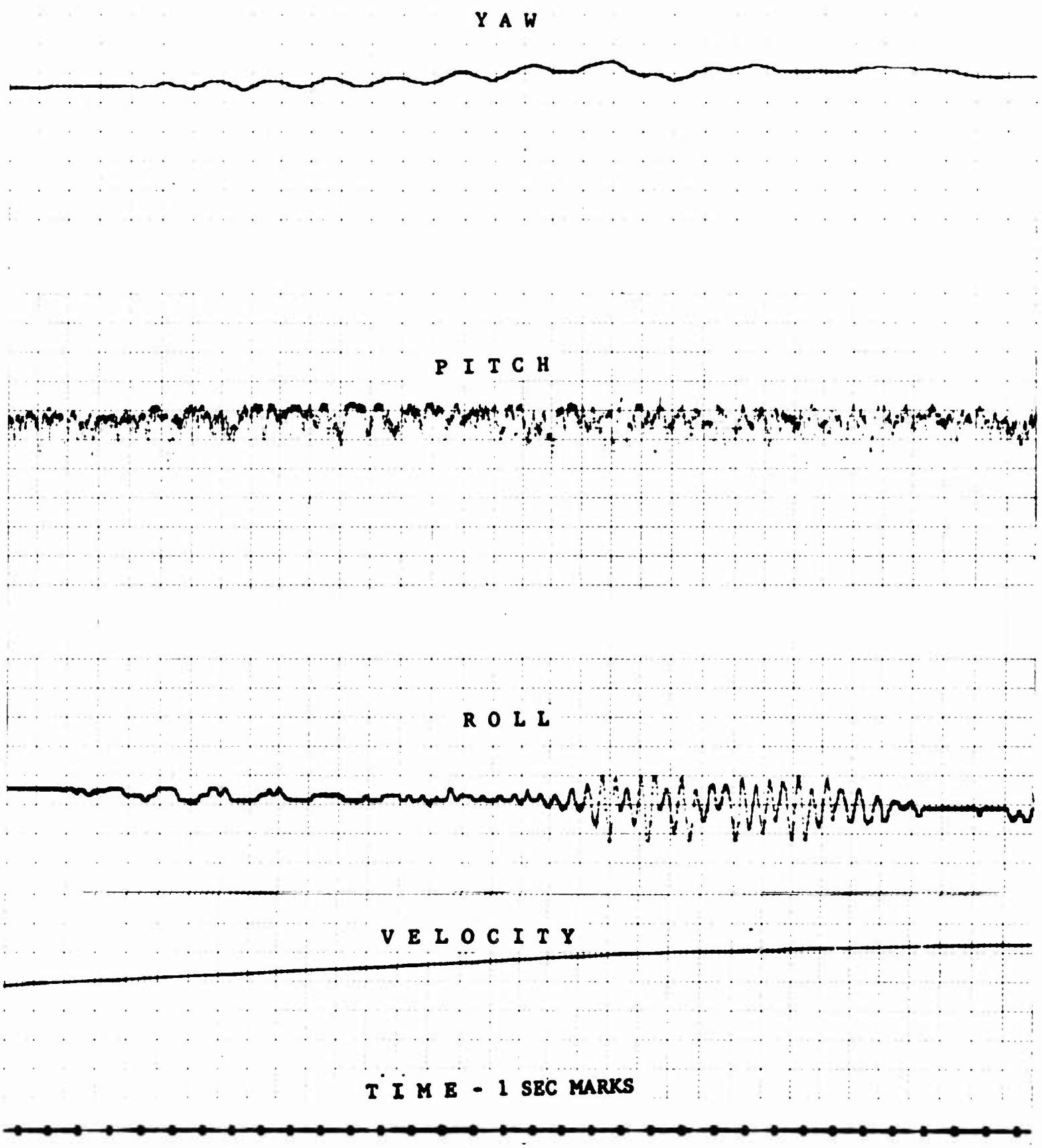

FIGURE 11. Dynamic Behavior of Winged GEM Model - Code 5.

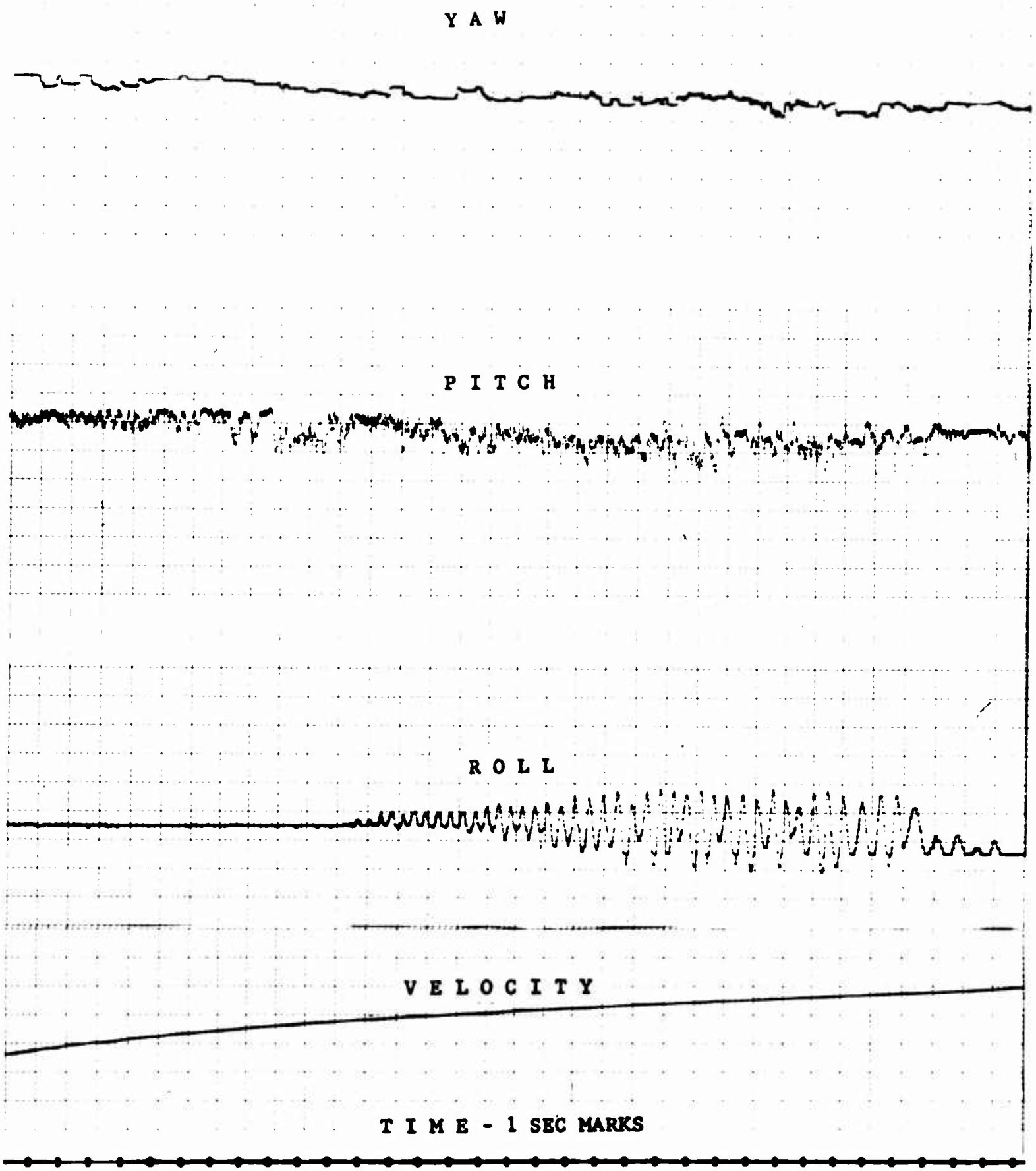

FIGURE 12. Dynamic Behavior of Winged GEM Model - Code 6.

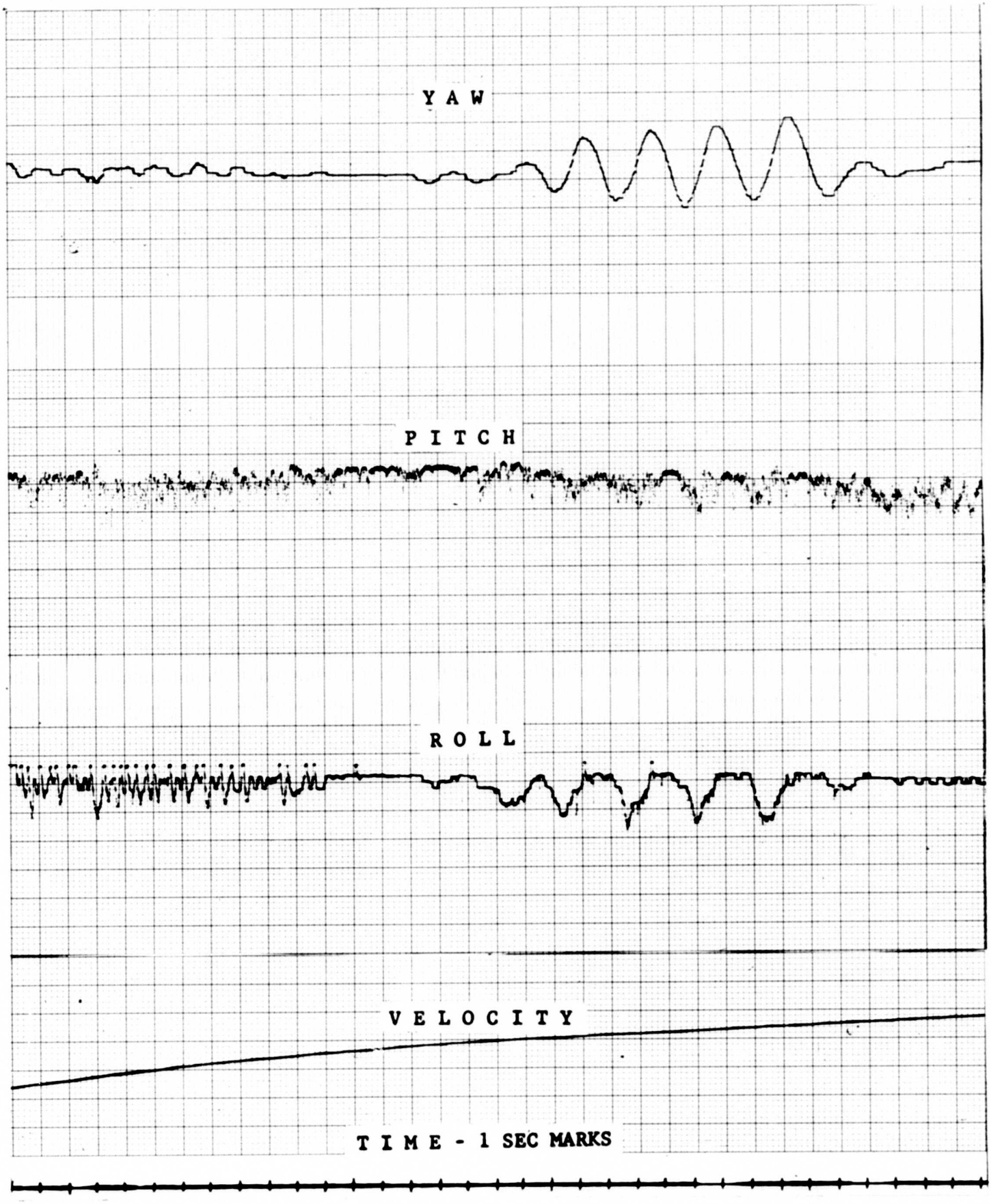

FIGURE 13. Dynamic Behavior of Winged GEM Model - Code 7.

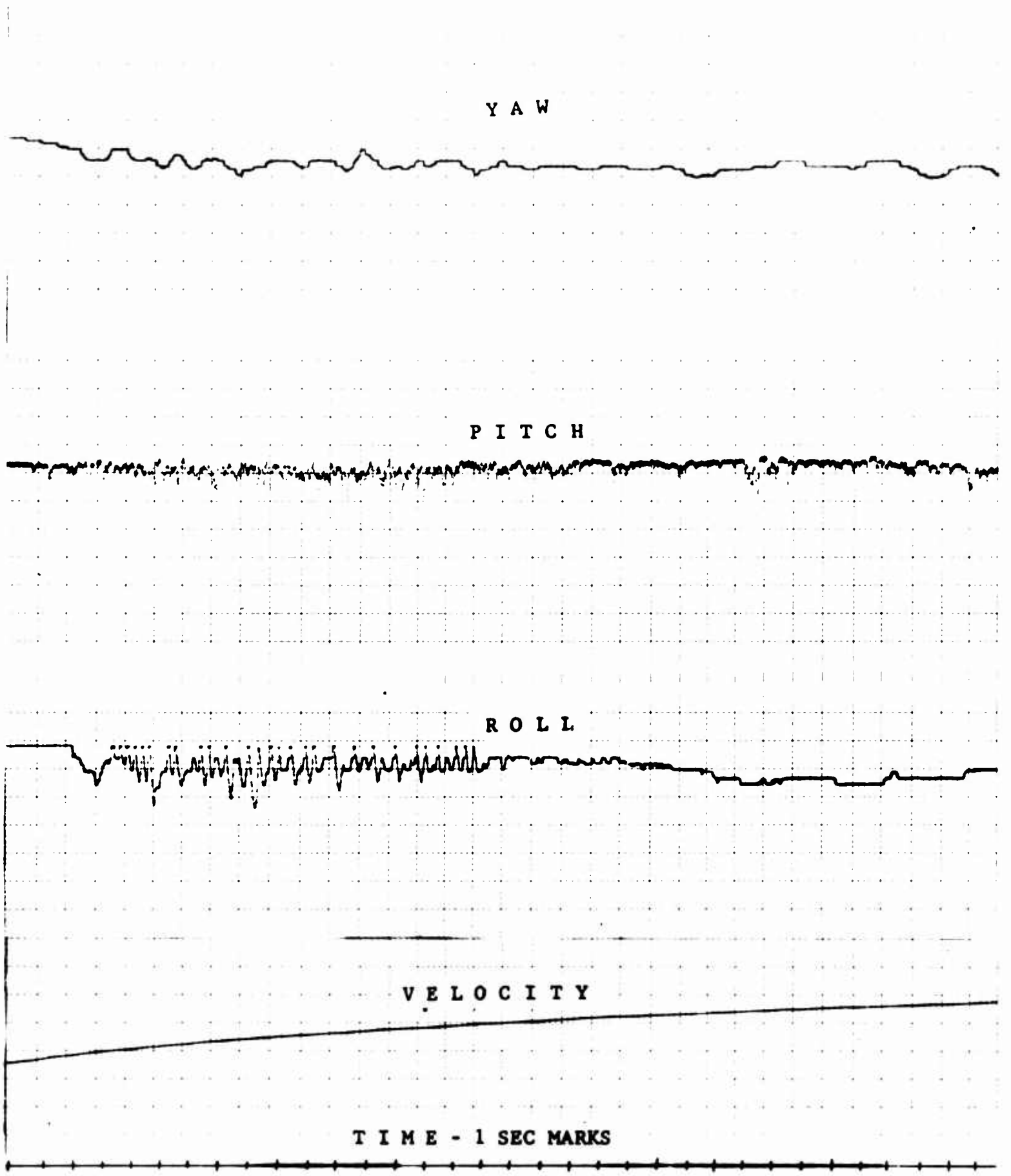

FIGURE 14. Dynamic Behavior of Winged GEM Model - Code 8.

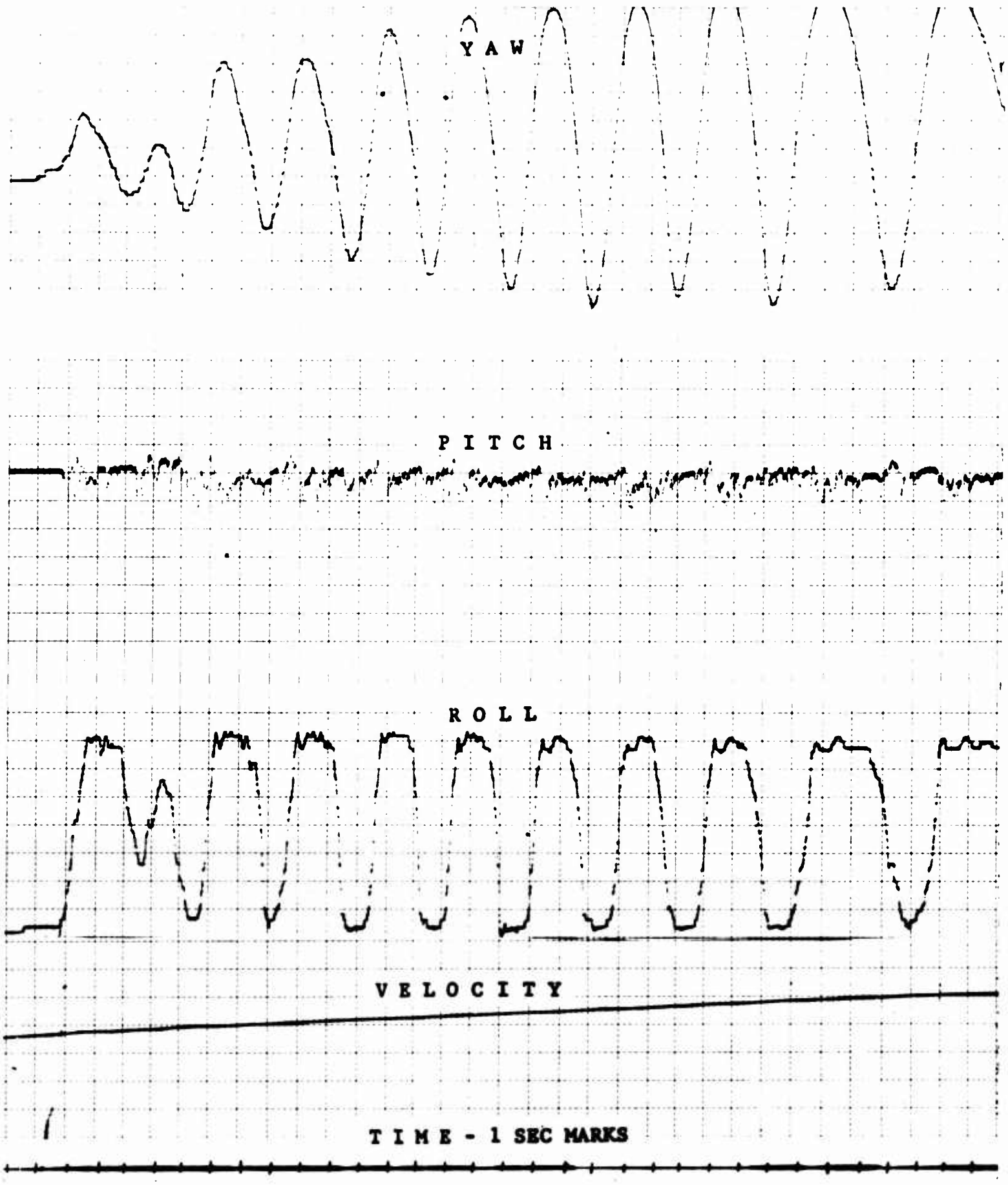

FIGURE 15. Dynamic Behavior of Winged GEM Model • Code 9.

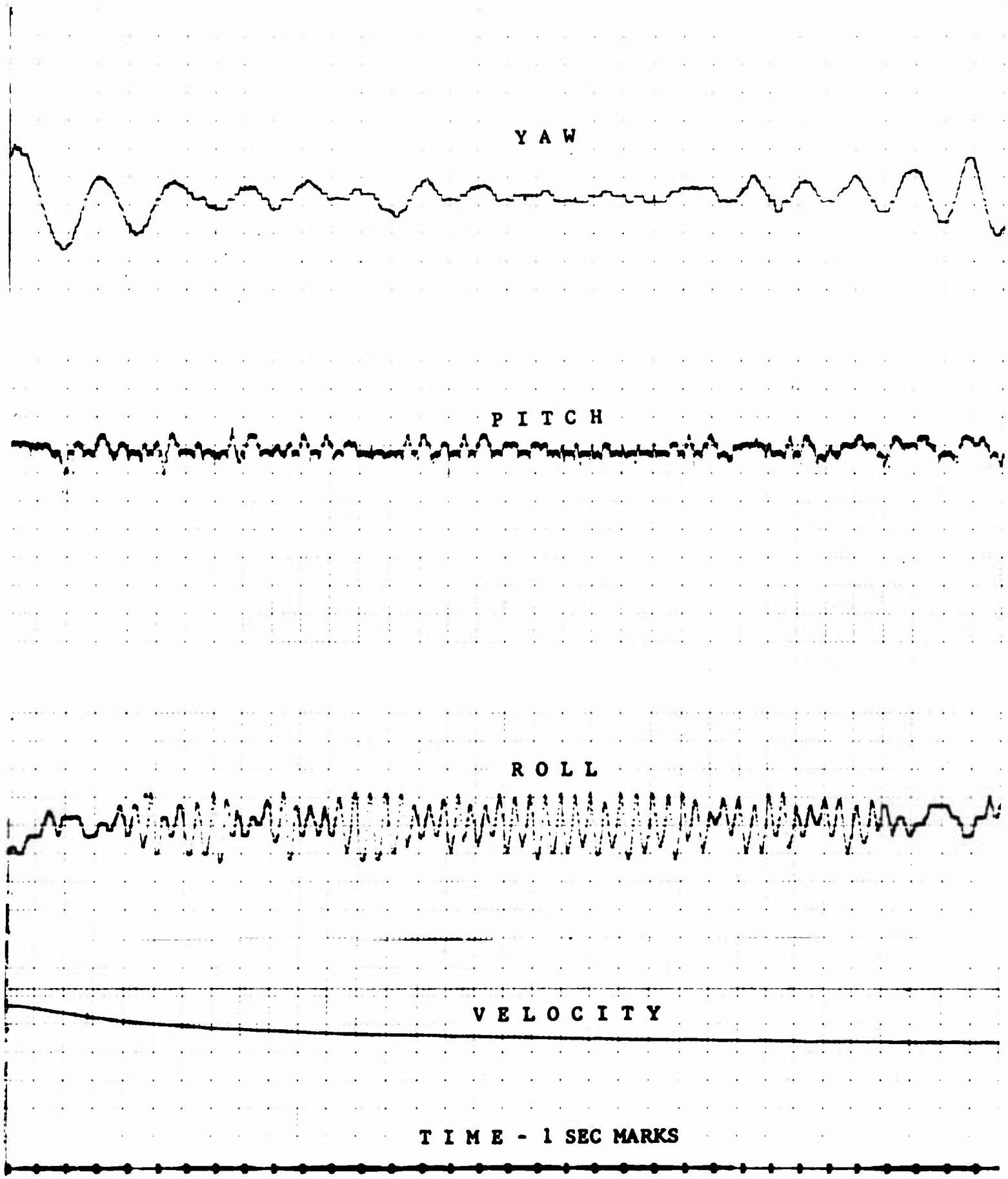

FIGURE 16. Dynamic Behavior of Winged GEM Model - Code 10.

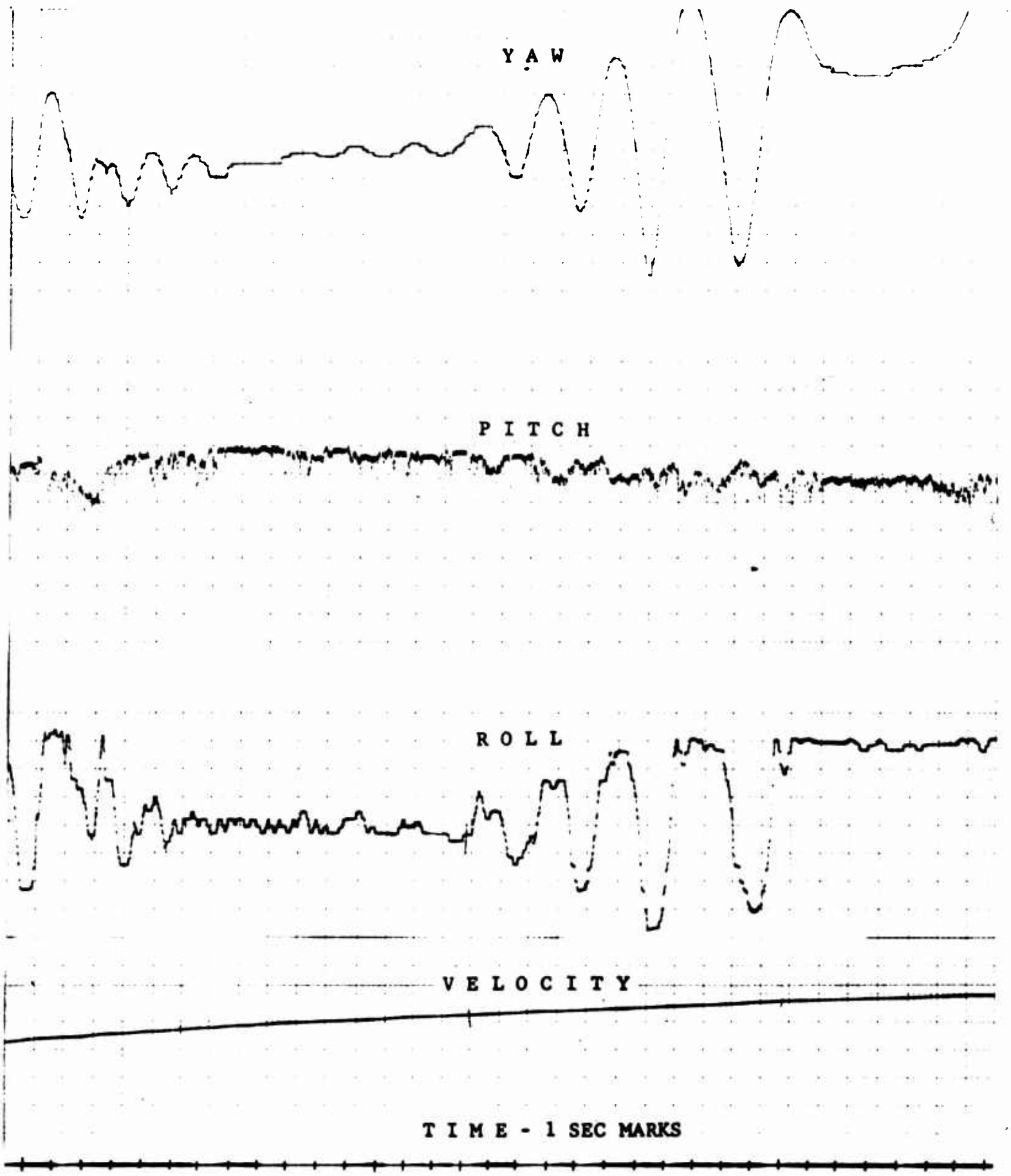

FIGURE 17. Dynamic Behavior of Winged GEM Model - Code 11.

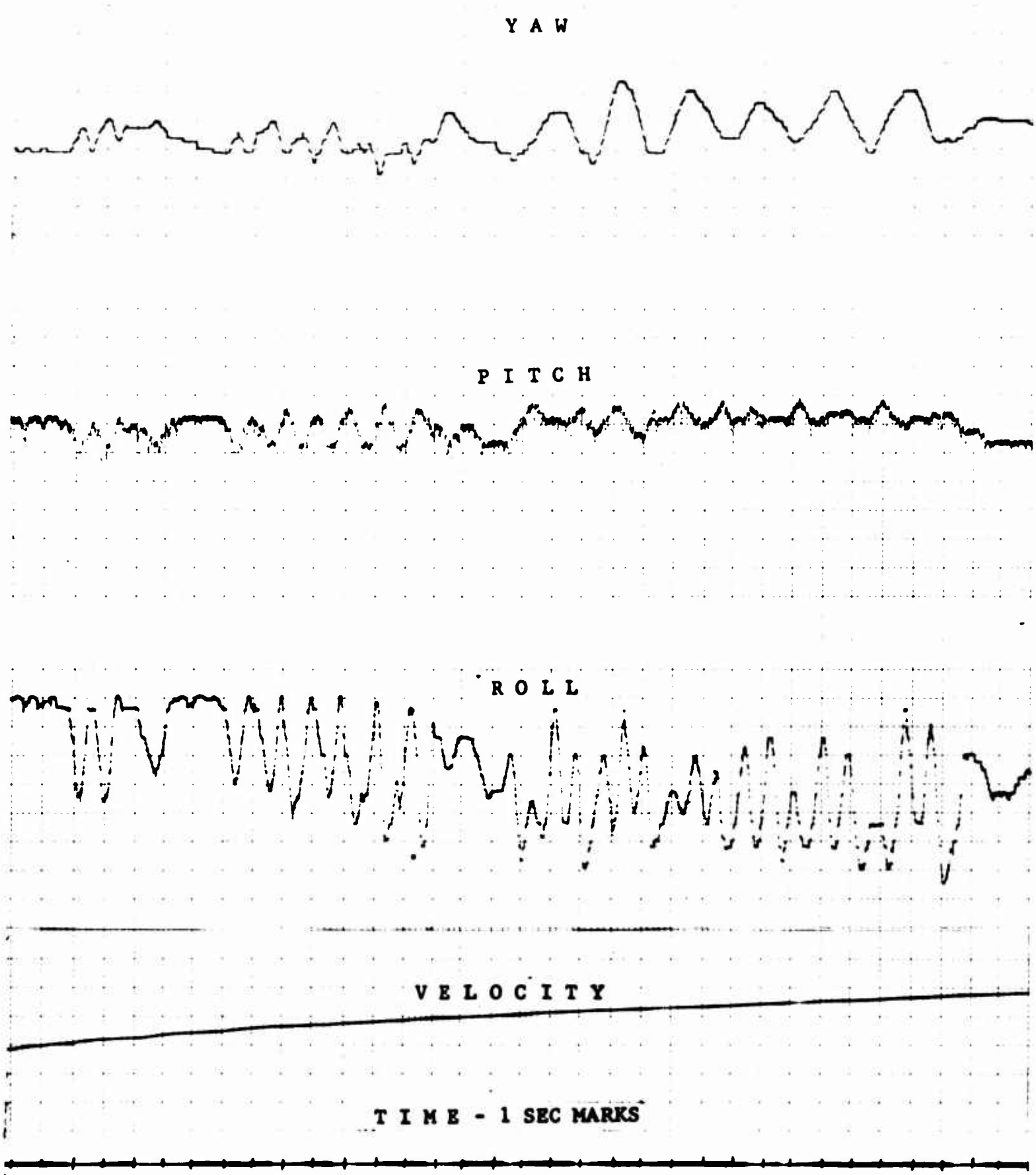

FIGURE 18. Dynamic Behavior of Winged GEM Model - Code 12.

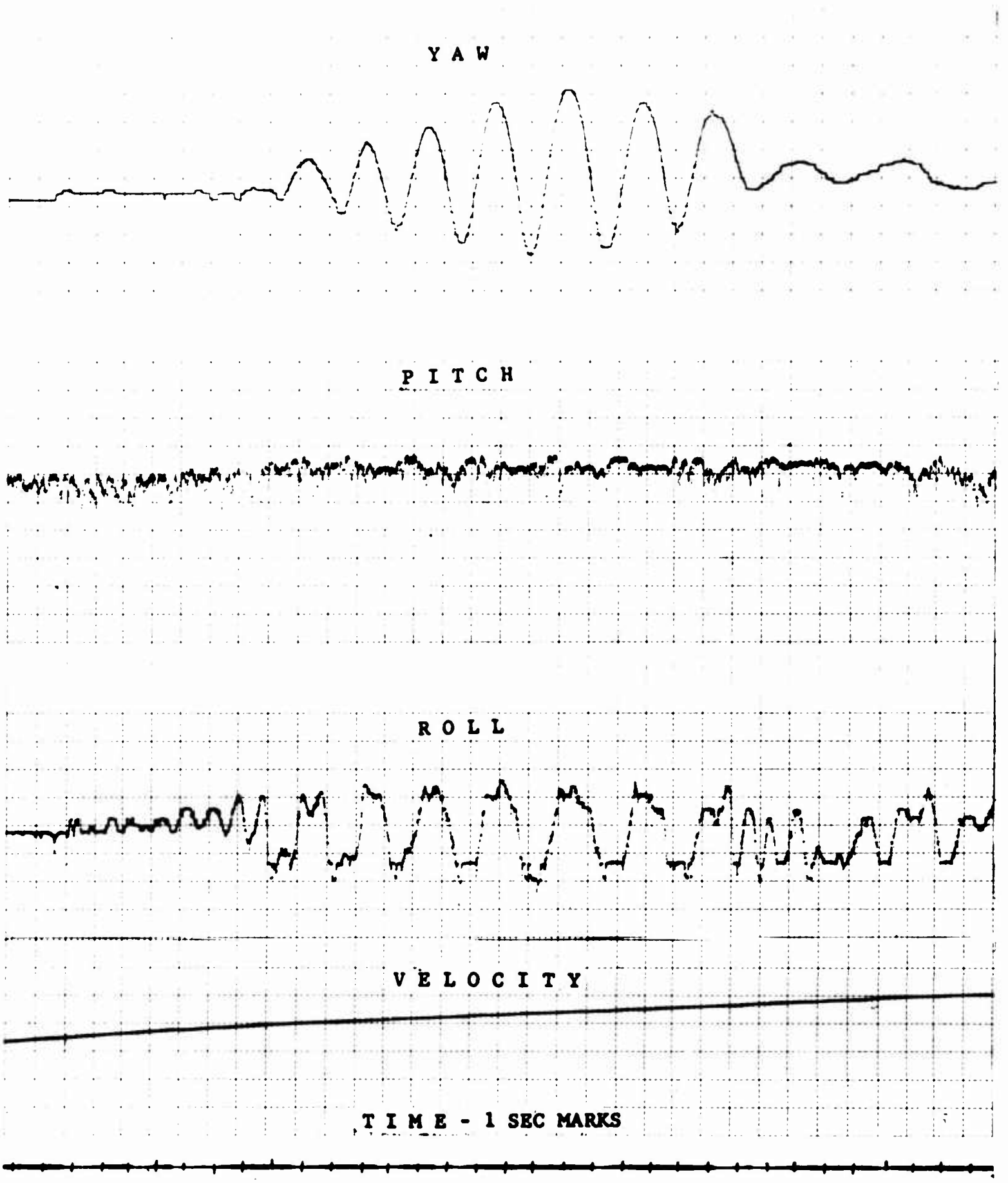

FIGURE 19. Dynamic Behavior of Winged GEM Model 4 Code 13.

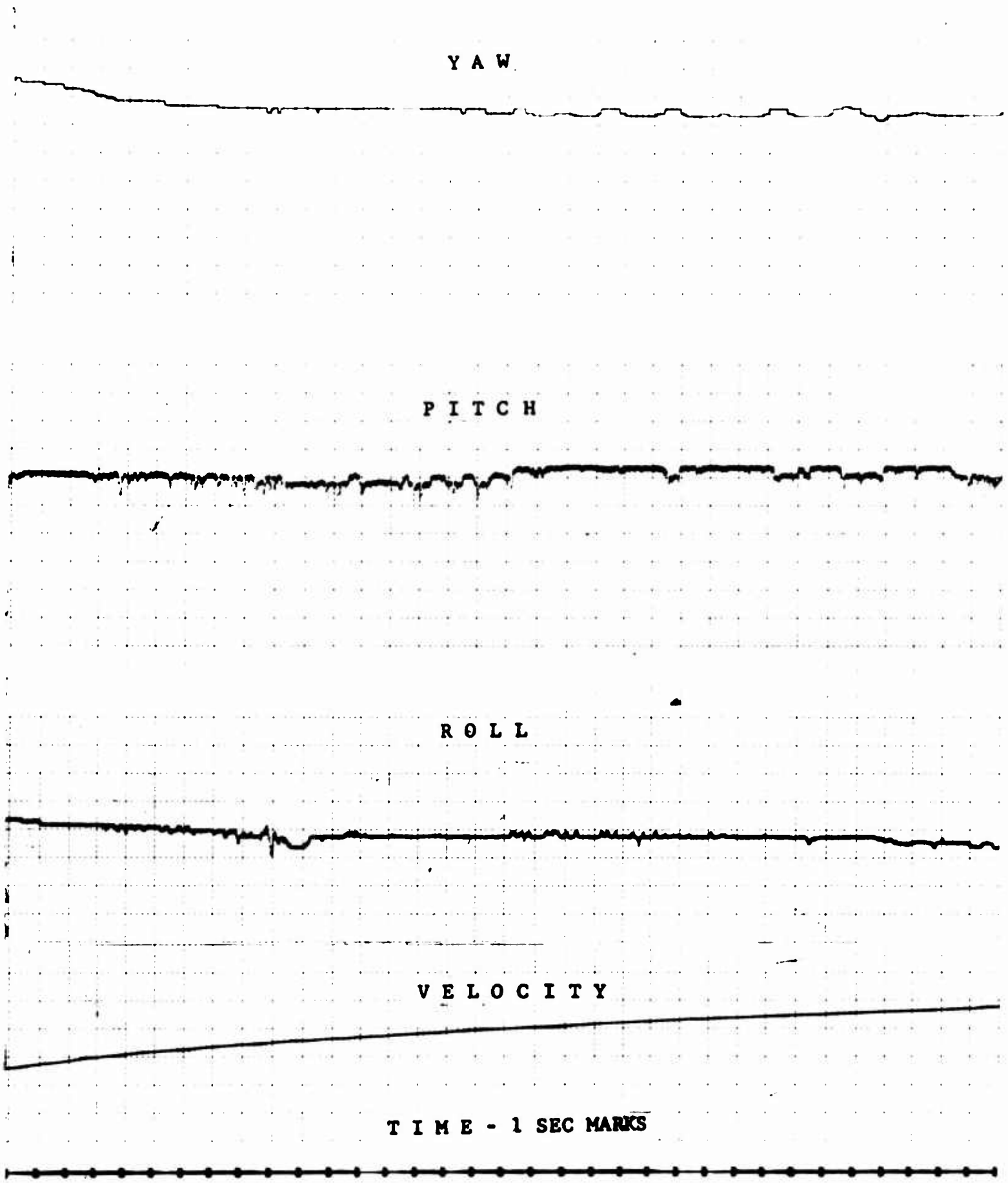

FIGURE 20. Dynamic Behavior of Winged GEM Model - Code 14.

A Summary of the Dynamic Behaviour of the Various Configurations Tested			
Code	Variable	Wing Type	Constant
1 2	low C_μ high C_μ	no wing	h/mac = .05
2 3	h/mac = .05 h/mac = .025	no wing	high C_μ
4 5	h/mac = .05 h/mac = .025	swept wing	high C_μ high wing, c.g. @ .25 mac
5 6	c.g. @ .25 mac c.g. @ .00 mac	swept wing	high C_μ h/mac = .025 high wing, δ/mac = .35
6 7	high wing δ/mac = .35 low wing δ/mac = .10	swept wing	high C_μ h/mac = .025 c.g. @ .00 mac
7 8	high C_μ low C_μ	swept wing	h/mac = .025 low wing, δ/mac = .10 c.g. @ .00 mac
9 10	low C_μ high C_μ	straight wing	h/mac = .05 high wing, δ/mac = .35 c.g. @ .00 mac
10 11	high wing δ/mac = .35 low wing δ/mac = .10	straight wing	h/mac = .05 high C_μ c.g. @ .00 mac
11 12	c.g. @ .00 mac c.g. @ .25 mac	straight wing	h/mac = .05 high C_μ low wing, δ/mac = .10
12 13	h/mac = .05 h/mac = .025	straight wing	high C_μ low wing, δ/mac = .10 c.g. @ .25 mac
14	--	straight wing	low C_μ, h/mac = .05 c.g. @ .5 mac very high wing, δ/mac = .45

FIGURE 21. Summary of Dynamic Behavior of Winged GEM Model.

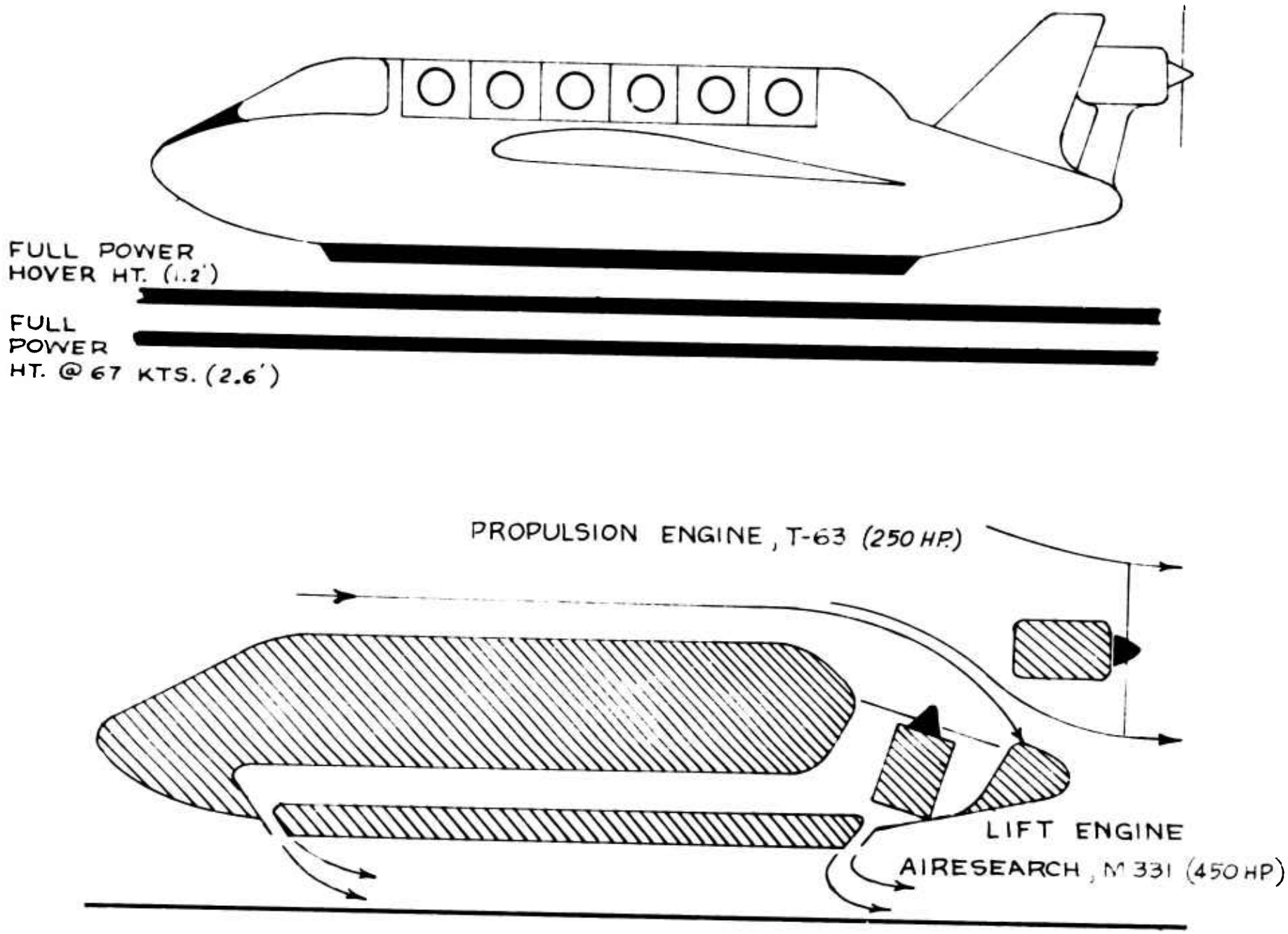

FIGURE 22. General Layout Optimized Winged GEM.

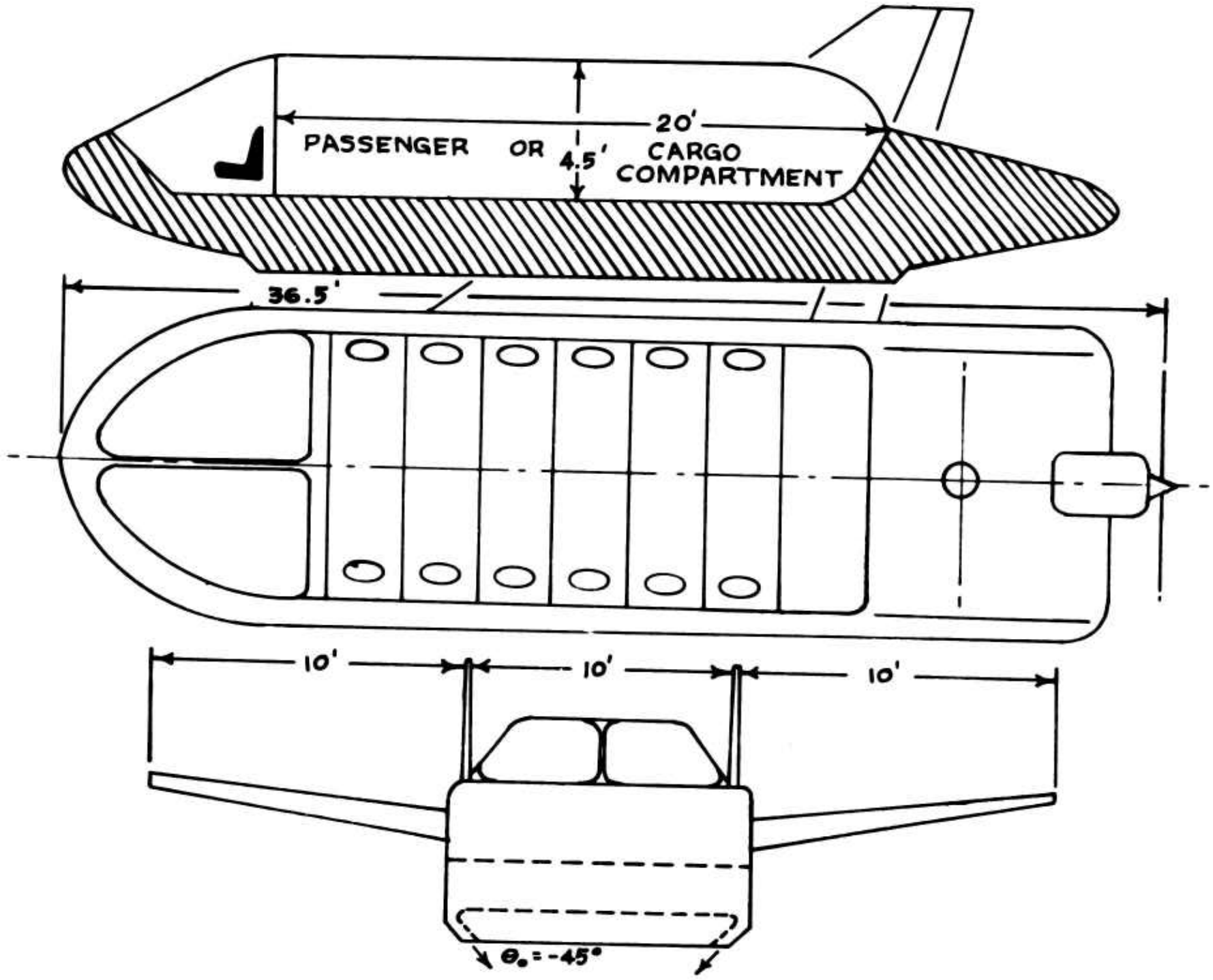

FIGURE 22 contd. General Layout Optimized Winged GEM.

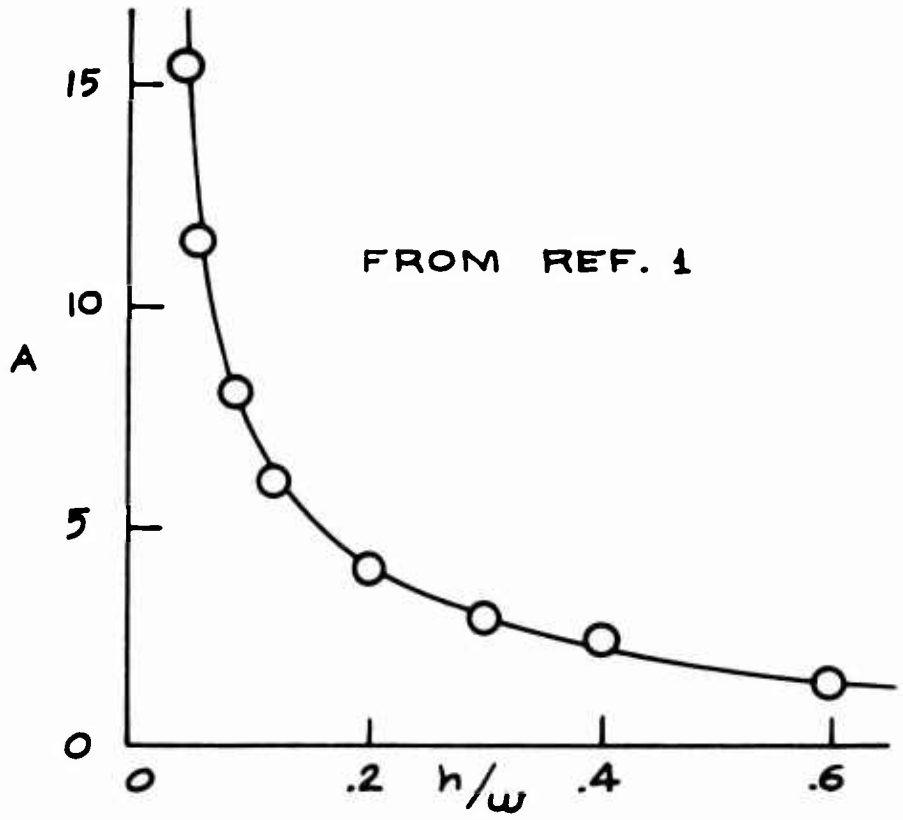

FIGURE 23. Estimated Augmentation Curve - Hovering Case.

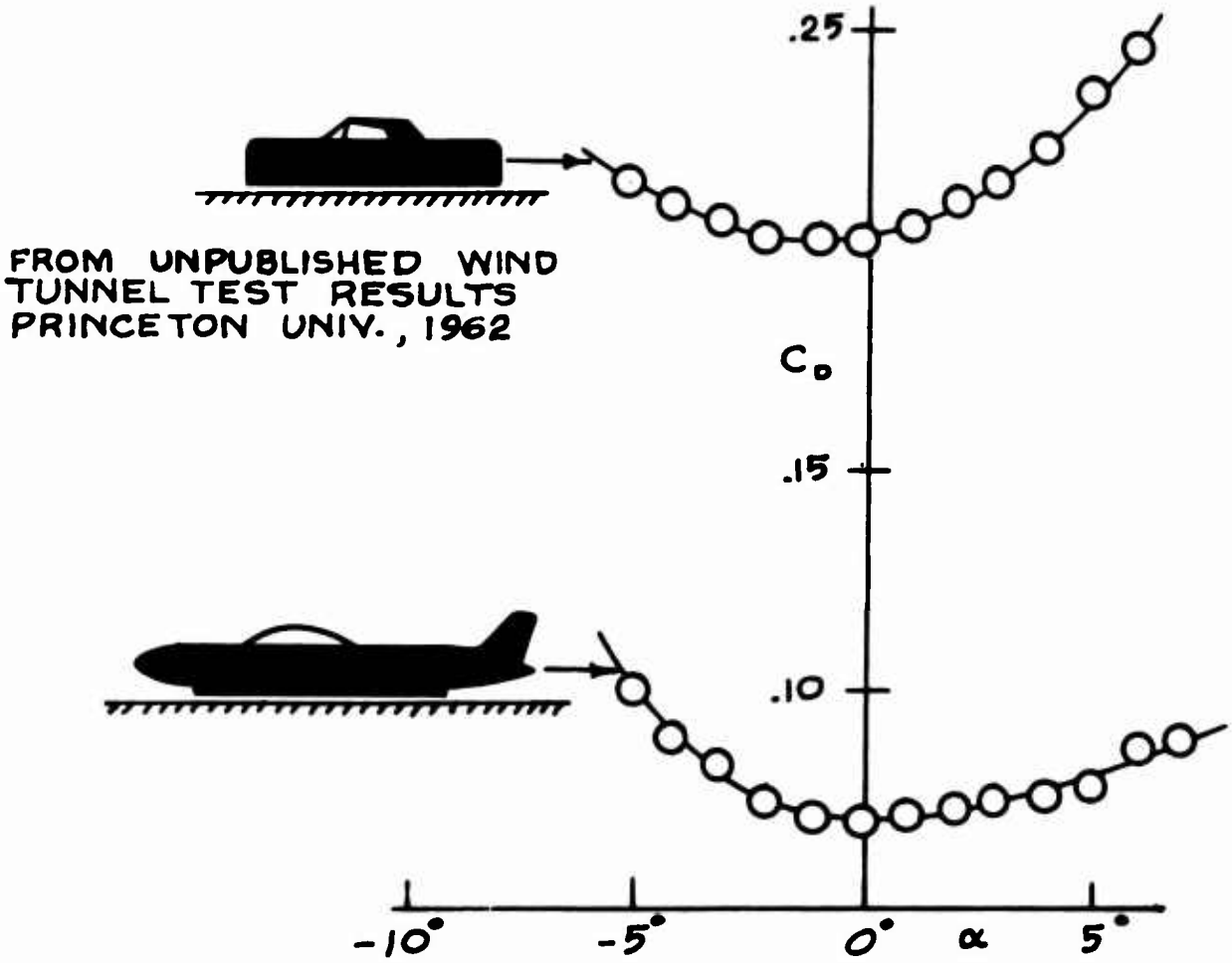

FIGURE 24. Power Off Drag Characteristics of C-W Air Car.

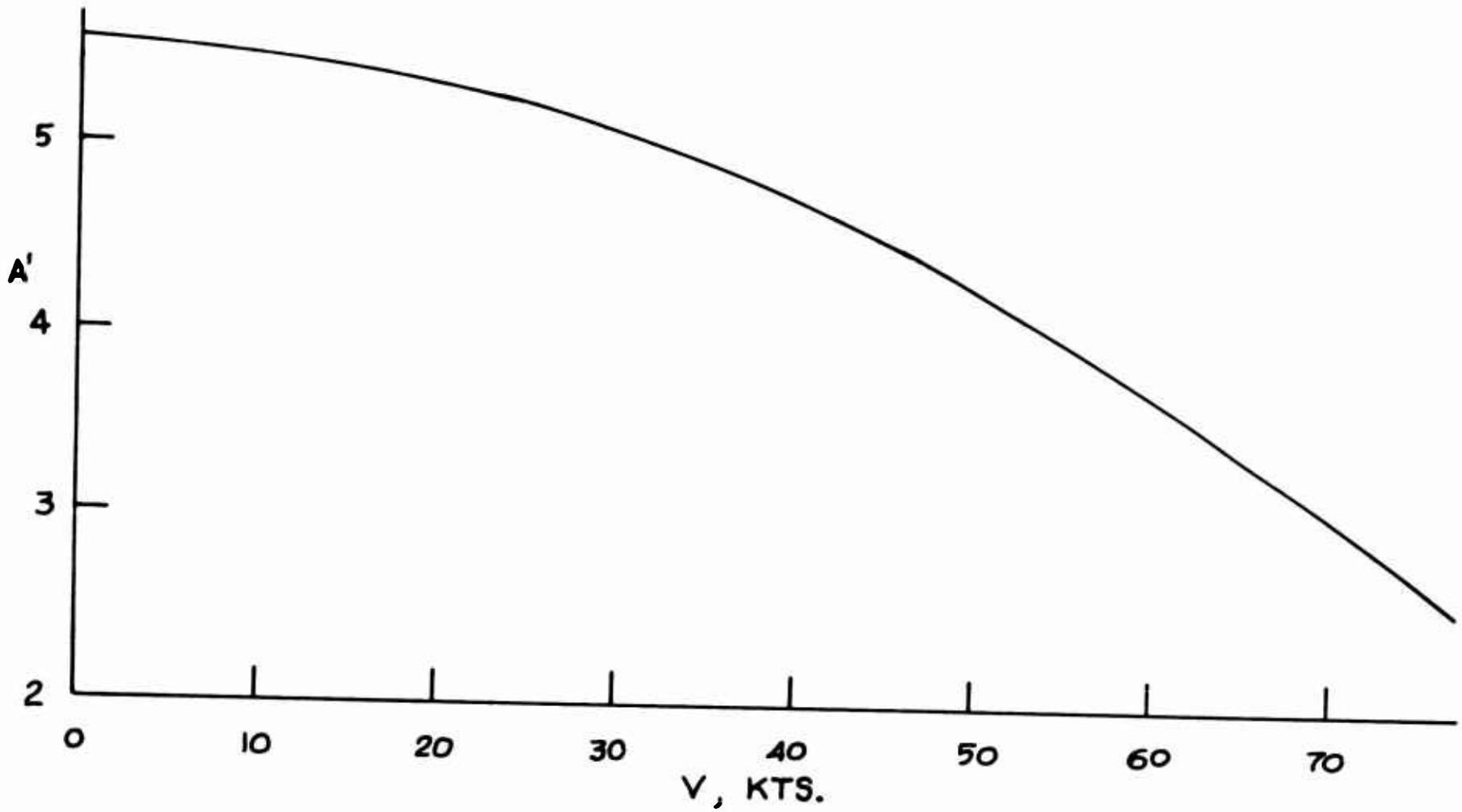

FIGURE 25. Effect of Velocity on Augumentation Ratio (Wings Deployed - 100% Throttle).

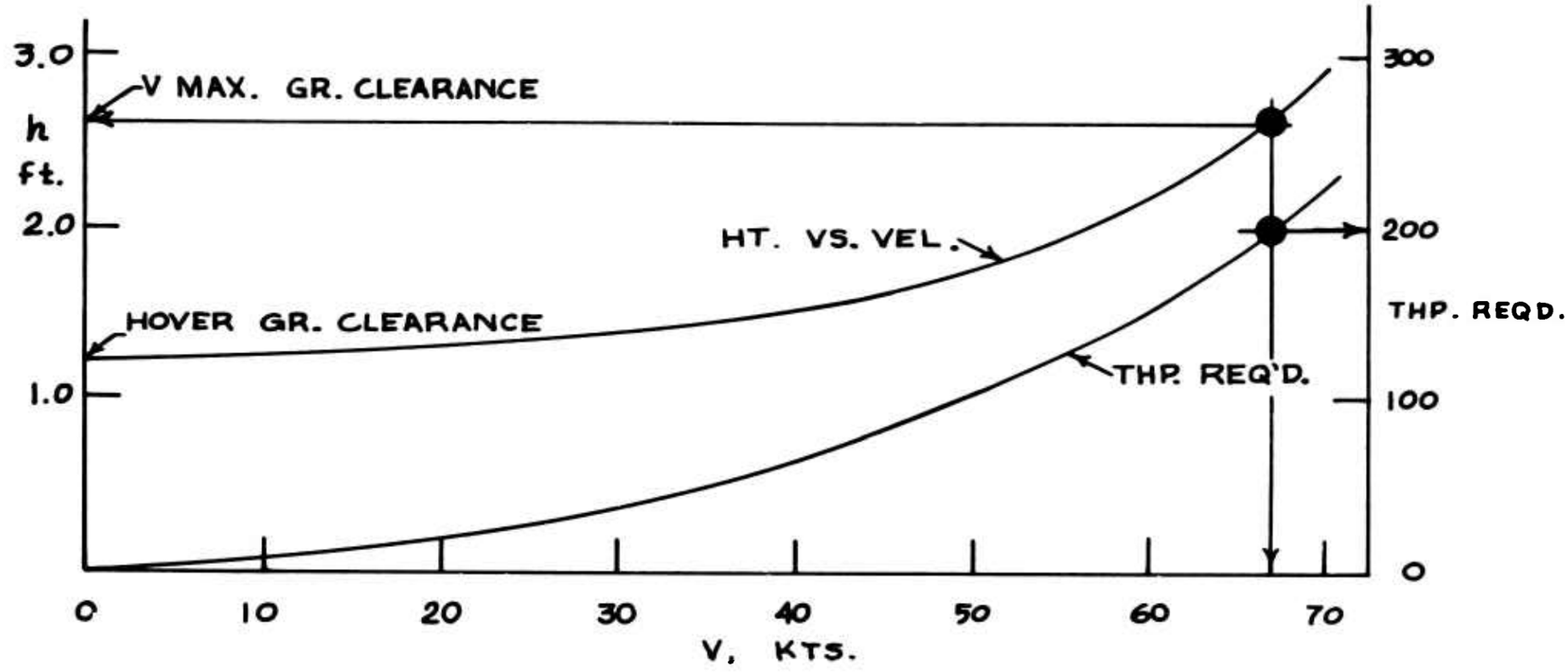

FIGURE 26. Speed, Height, Power Relationship (Wings Deployed)

BLANK PAGE

Unclassified
Security Classification

DOCUMENT CONTROL DATA - R&D

(Security classification of title, body of abstract and indexing annotation must be entered when the overall report is classified)

1 ORIGINATING ACTIVITY (Corporate author)
Princeton University
Princeton, New Jersey

2a REPORT SECURITY CLASSIFICATION
Unclassified

2b GROUP

3 REPORT TITLE
AN INVESTIGATION OF A DYNAMIC INSTABILITY OF A WINGED GEM

4 DESCRIPTIVE NOTES (Type of report and inclusive dates)

5 AUTHOR(S) (Last name, first name, initial)
Condit, P. M., and Harrington, J. E.

6 REPORT DATE	7a TOTAL NO OF PAGES	7b NO OF REFS
December 1964	46	4

8a CONTRACT OR GRANT NO	9a ORIGINATOR'S REPORT NUMBER(S)
DA 44-177-AMC-64(T)	USATRECOM 64-54
b PROJECT NO Task 1D021701A04802	
c	9b OTHER REPORT NO(S) (Any other numbers that may be assigned this report)
d	692

10 AVAILABILITY/LIMITATION NOTICES
Qualified requesters may obtain copies of this report from DDC.
This report has been furnished to the Department of Commerce for sale to the public.

11 SUPPLEMENTARY NOTES	12 SPONSORING MILITARY ACTIVITY
	U.S. Army Transportation Research Command Fort Eustis, Va.

13 ABSTRACT
An experimental investigation of the lateral dynamic stability characteristics of a winged GEM. The causes of instability are determined and a method of correcting the condition proposed.

DD FORM 1 JAN 64 1473

Unclassified
Security Classification

14 KEY WORDS	LINK A		LINK B		LINK C	
	ROLE	WT	ROLE	WT	ROLE	WT

INSTRUCTIONS

1. **ORIGINATING ACTIVITY**: Enter the name and address of the contractor, subcontractor, grantee, Department of Defense activity or other organization *(corporate author)* issuing the report.

2*a*. **REPORT SECURITY CLASSIFICATION**: Enter the overall security classification of the report. Indicate whether "Restricted Data" is included. Marking is to be in accordance with appropriate security regulations.

2*b*. **GROUP**: Automatic downgrading is specified in DoD Directive 5200.10 and Armed Forces Industrial Manual. Enter the group number. Also, when applicable, show that optional markings have been used for Group 3 and Group 4 as authorized.

3. **REPORT TITLE**: Enter the complete report title in all capital letters. Titles in all cases should be unclassified. If a meaningful title cannot be selected without classification, show title classification in all capitals in parenthesis immediately following the title.

4. **DESCRIPTIVE NOTES**: If appropriate, enter the type of report, e.g., interim, progress, summary, annual, or final. Give the inclusive dates when a specific reporting period is covered.

5. **AUTHOR(S)**: Enter the name(s) of author(s) as shown on or in the report. Enter last name, first name, middle initial. If military, show rank and branch of service. The name of the principal author is an absolute minimum requirement.

6. **REPORT DATE**: Enter the date of the report as day, month, year, or month, year. If more than one date appears on the report, use date of publication.

7*a*. **TOTAL NUMBER OF PAGES**: The total page count should follow normal pagination procedures, i.e., enter the number of pages containing information.

7*b*. **NUMBER OF REFERENCES**: Enter the total number of references cited in the report.

8*a*. **CONTRACT OR GRANT NUMBER**: If appropriate, enter the applicable number of the contract or grant under which the report was written.

8*b*, 8*c*, & 8*d*. **PROJECT NUMBER**: Enter the appropriate military department identification, such as project number, subproject number, system numbers, task number, etc.

9*a*. **ORIGINATOR'S REPORT NUMBER(S)**: Enter the official report number by which the document will be identified and controlled by the originating activity. This number must be unique to this report.

9*b*. **OTHER REPORT NUMBER(S)**: If the report has been assigned any other report numbers *(either by the originator or by the sponsor)*, also enter this number(s).

10. **AVAILABILITY/LIMITATION NOTICES**: Enter any limitations on further dissemination of the report, other than those imposed by security classification, using standard statements such as:

(1) "Qualified requesters may obtain copies of this report from DDC."

(2) "Foreign announcement and dissemination of this report by DDC is not authorized."

(3) "U. S. Government agencies may obtain copies of this report directly from DDC. Other qualified DDC users shall request through _____."

(4) "U. S. military agencies may obtain copies of this report directly from DDC. Other qualified users shall request through _____."

(5) "All distribution of this report is controlled. Qualified DDC users shall request through _____."

If the report has been furnished to the Office of Technical Services, Department of Commerce, for sale to the public, indicate this fact and enter the price, if known.

11. **SUPPLEMENTARY NOTES**: Use for additional explanatory notes.

12. **SPONSORING MILITARY ACTIVITY**: Enter the name of the departmental project office or laboratory sponsoring *(paying for)* the research and development. Include address.

13. **ABSTRACT**: Enter an abstract giving a brief and factual summary of the document indicative of the report, even though it may also appear elsewhere in the body of the technical report. If additional space is required, a continuation sheet shall be attached.

It is highly desirable that the abstract of classified reports be unclassified. Each paragraph of the abstract shall end with an indication of the military security classification of the information in the paragraph, represented as *(TS)*, *(S)*, *(C)*, or *(U)*.

There is no limitation on the length of the abstract. However, the suggested length is from 150 to 225 words.

14. **KEY WORDS**: Key words are technically meaningful terms or short phrases that characterize a report and may be used as index entries for cataloging the report. Key words must be selected so that no security classification is required. Identifiers, such as equipment model designation, trade name, military project code name, geographic location, may be used as key words but will be followed by an indication of technical context. The assignment of links, rules, and weights is optional.